# Influence of geometrical imperfections and residual stresses on the reliability of high strength steel welded I-section columns using Monte Carlo simulation

Ferreira Filho, José Osvaldo; da Silva, Luís Simões; Tankova, Trayana; Carvalho, Hermes

**DOI**
10.1016/j.jcsr.2024.108548

**Publication date**
2024

**Document Version**
Final published version

**Published in**
Journal of Constructional Steel Research

Journal of Constructional Steel Research 215 (2024) 108548

Contents lists available at ScienceDirect

Journal of Constructional Steel Research

journal homepage: www.elsevier.com/locate/jcsr

# Influence of geometrical imperfections and residual stresses on the reliability of high strength steel welded I-section columns using Monte Carlo simulation

José Osvaldo Ferreira Filho [a,*], Luís Simões da Silva [a], Trayana Tankova [b], Hermes Carvalho [c,d]

[a] University of Coimbra, ISISE, ARISE, Department of Civil Engineering, Coimbra, Portugal
[b] Delft University of Technology, Department of Engineering Structures, Delft, Netherlands
[c] Federal University of Minas Gerais, Department of Structural Engineering, Belo Horizonte, Minas Gerais, Brazil
[d] Department of Structural Engineering and Geotechnical, University of São Paulo, Brazil

ARTICLE INFO

*Keywords:*
High strength steel
Buckling resistance of columns
Reliability analysis
Monte Carlo simulation
Eurocode 3

ABSTRACT

This paper aims to assess the influence of geometrical imperfections and residual stresses on the reliability of the stability design rules for steel columns in Eurocode 3 considering a full probabilistic approach and further validate the new buckling curves in the scope of the ongoing revision of the Structural Eurocodes. A reliability assessment of major- and minor-axis flexural buckling of high-strength steel (HSS) welded I-section columns was performed, considering all basic variables as random, including the geometrical and material imperfections, in addition to the material properties of steel and the geometry of the cross-section. An advanced finite element model calibrated with experimental test results is used to perform a very large (290,126 simulations) parametric study covering the majority of practical geometries. Subsequently, Monte Carlo simulation is used to estimate the design values of the buckling resistance that correspond to the target probability of failure of the Eurocodes. Finally, these values are compared to the proposed buckling curves for HSS columns, showing good agreement and supporting their adoption in the revised EN 1993–1-1. It is also concluded that it is on the safe side to carry out a reliability assessment with deterministic reference values for structural imperfections.

## 1. Introduction

The progressive widespread availability of HSS with appropriate weldability and ductility for structural applications has stirred the extension of design rules to steel grades with yield strengths reaching 1000 MPa. In Europe, this enlarged scope was implemented in 2 stages: in 2007, EN 1993–1-12 [1], allowed the use of HSS with steel grades up to S700, while there is ongoing work on prEN 1993–1-12 to further extend this range up to S960. This trend was obviously replicated outside Europe, namely in the American [3] and Chinese [4] codes.

Concerning the buckling resistance of members, due to the lack of experimental evidence at the time of its publication, EN 1993–1-12 [1] adopted conservative approaches by maintaining the buckling curves that were prescribed for S460 for higher steel grades, despite the well-known beneficial effect of residual stresses with increasing steel grade. Historically, the establishment of the European buckling curves in the 1960's and early 1970's for compressed columns [5–7], pioneered the use of probabilistic assessments to validate the choice of buckling curves. Specifically, Strating and Vos [7] carried out Monte Carlo assessments using statistical distributions for the relevant basic variables directly obtained from the large set of experimental tests that were undertaken, including geometrical imperfections (bow imperfection) and residual stresses. It is noted that their assessment was linked to a notional target probability of failure corresponding to the 5% percentile. Since then, several investigations aimed to evaluate the level of safety provided by Eurocode 3. During the various stages of the preparation of the Eurocodes (ENV and EN versions), several statistical assessments and research projects were carried out to try to establish an adequate safety level for steel members and connections, in line with the target failure probability of $10^{-4}$ [8,9]. However, these studies never unequivocally established which partial factor, $\gamma_M$, should be adopted to ensure that the target failure probability is met [10,11].

Recently, the SAFEBRICTILE project [12] reassessed the reliability level of the Eurocode 3 design rules by providing a consistent procedure for the safety assessment of the various failure modes for steel structures.

* Corresponding author at: Department of Civil Engineering, University of Coimbra, Polo II, Pinhal de Marrocos, 3030-290 Coimbra, Portugal.
*E-mail address:* jose.filho@dec.uc.pt (J.O. Ferreira Filho).

https://doi.org/10.1016/j.jcsr.2024.108548
Received 12 September 2023; Received in revised form 23 January 2024; Accepted 11 February 2024
Available online 15 February 2024

**Notations**

*Lowercase Latin letters*

| | |
|---|---|
| $b$ | *Width of the cross-section* |
| $c$ | Outstand flange width |
| $c_f$ | *appropriate outstand width of the flange plate* |
| $c_w$ | *appropriate outstand width of the web* |
| $d$ | *Depth of the web plate* |
| $e_0$ | *amplitude of the initial geometric imperfection* |
| $f_y$ | Yield stress |
| $f_u$ | *Ultimate Stress* |
| $h$ | Depth of the cross-section |
| $r_k$ | *characteristic value or theoretical value of the resistance* |
| $r_d$ | design values of the resistance |
| $t_f$ | Thickness of the flange |
| $t_w$ | Thickness of the web |
| $x$-$x$ | Axis along the member |
| $y$-$y$ | Cross section major-axis |
| $z$-$z$ | Cross section minor-axis |

*Uppercase Latin letters*

| | |
|---|---|
| $A$ | Gross area of the cross-section |
| $A_{eff}$ | Effective area of the cross-section |
| $A_f$ | Gross area of the flange |
| $A_w$ | Gross area of the web |
| $E$ | Modulus of elasticity or Young's modulus and Action variable |
| $L$ | Length of the member |
| $N_{b,Rd}$ | *Buckling resistance of a compression member* |
| $N_{cr}$ | Elastic critical force |
| $P_f$ | *Probability of Failure* |
| $R$ | *Resistance variable* |

*Lowercase Greek letters*

| | |
|---|---|
| $\alpha$ | Imperfection factor |
| $\alpha_E$, $\alpha_R$ | Sensitivity factors to measure the relative importance of the random variables related to the resistance, R, and action, E, sides, respectively |
| $\gamma_M$ | Partial factor |
| $\gamma_{M1}$ | Partial factor for the verification of the buckling resistance of members acc. to Eurocode 3 |
| $\gamma_{M1}{}^*$ | Required partial factor |
| $\varepsilon$ | Material parameter depending on $f_y$ |
| $\overline{\lambda}$ | Relative slenderness for flexural buckling |
| $\overline{\lambda}_\rho$ | Relative plate slenderness for plate buckling |
| $\rho_f$; $\rho_w$ | Reduction factors for plate buckling related to flanges and web, respectively |
| $\sigma_E$, $\sigma_R$ | *Standard deviation of the random variables related to the resistance, R, and action, E, sides, respectively* |
| $\boldsymbol{\sigma}_{f,c}$ | *Compression residual stresses of the flanges* |
| $\boldsymbol{\sigma}_{f,t}$ | *Tension residual stresses of the flanges* |
| $\boldsymbol{\sigma}_{w,c}$ | Compression residual stresses of the web |
| $\boldsymbol{\sigma}_{w,t}$ | Tension residual stresses of the web |
| $\phi$ | Buckling parameter to determine the reduction factor for flexural buckling |
| $\chi$ | Reduction factor |

*Uppercase Greek letters*

| | |
|---|---|
| $\beta$ | Reliability index to establish the target reliability level |
| $\Phi$ | Cumulative distribution function (CDF) for the standard normal distribution |

Statistical distributions of relevant basic variables were suggested for the calibration of design rules that were included in Annex E of FprEN1993–1-1 [13]. This reassessment was carried out using the Annex D procedure with the detailed specifications of Tankova et al. [14], whereby the geometrical and material imperfections were assumed with reference deterministic values. Subsequently, the STROBE project [15] addressed the buckling resistance of HSS members with steel grades ranging from S460 to S700. An experimental campaign was carried out, accompanied by a large parametric study and the proposal of improved design rules matching the target probability of failure [16–18]. Additionally, the statistical characterization of residual stresses was also addressed [19], leading to a new residual stress model that is more accurate and with less scatter [20]. Outside Europe, many research projects including experimental tests were also carried out [21–31], providing further reliable data to support the adoption of more accurate design models.

The validation of the above results assuming that all relevant basic variables are defined as random variables in the context of a full probabilistic reliability assessment is desired, as it was done in the 1970s by Strating and Vos [7].

In this paper, the reliability assessment of the stability design rules for major- and minor-axis flexural buckling of S690 high strength steel (HSS) welded I-section members is addressed. Firstly, an advanced finite element model calibrated with experimental test results is used to perform a very large parametric study covering simply supported columns with slenderness varying from 0.3 to 2.2. Secondly, material properties (yield strength, $f_y$, and Young's modulus, $E$) and cross section dimensions were stochastically modelled using the statistical distributions specified in Annex E of FprEN1993–1-1 [13], while the geometrical and material imperfections were modelled using recent statistical distributions obtained in the literature. The numerical analyses were divided into several groups of samples to evaluate the influence of the inclusion of the initial imperfections and residual stresses as random variables. Sensitivity analyses were also undertaken to evaluate the influence of different statistical parameters. From the results of around 290,126 advanced finite element analyses using the Monte Carlo method, design values were estimated for the buckling resistance that correspond to the target probability of failure of the Eurocodes. The results of the Monte Carlo reliability assessment were compared to the corresponding results from the reliability assessment of Tankova et al. [18], in which the Annex D [33] / SAFEBRICTILE [12] methodology was applied, proving that the latter approach yields safe-sided results. Finally, the design values were compared to the current design rules of Eurocode 3 [1,2,13] and to the new design rules from the proposed amendment [32] to FprEN1993–1-1 [13], further validating the proposed amendment [32] of the buckling curves for HSS welded I-section members.

## 2. Methodology

### 2.1. Scope

The objective of this assessment is the safety level of the resistance function of the flexural buckling of columns according to FprEN 1993–1-1 [13]. Since the problem is non-linear and involves several random variables, Monte Carlo simulation is used to estimate the corresponding failure probability and the recommendations of reliability verification from EN1990 [27] were followed *(see Section 5)*. Hence, as basic variables, cross-sectional dimensions (depth, $h$, width, $b$, and thickness of web and flanges, $t_w$ and $t_f$), material properties (yield stress, $f_y$, ultimate stress, $f_u$, and modulus of elasticity, $E$), and imperfections (initial geometric imperfections and residual stresses) were considered. Their

adopted statistical distributions are described in Section 3, and they were considered statistically independent [11].

Bearing in mind that the validity of the Monte Carlo simulation depends on the probability to be estimated, the following methodology was established:

- **STEP 1: Initial benchmarks:** (i) to select the sample size for each basic variable that is assumed as random [34]; (ii) to assess the influence of local buckling; and (iii) to study the influence of the residual stress pattern.
- **STEP 2: Sensitivity study:** to establish the influence of the randomness of the basic variables on the buckling resistance of columns. These sensitivity studies are performed for a single cross section to reduce the global number of numerical simulations.
- **STEP 3: Statistical assessment:** to define and implement a large parametric study for a representative set of cross sections, based on the conclusions of Step 2.

### 2.2. Basic variables and generation of samples

Table 1 summarizes the groups of samples used in the steps mentioned above. Groups 0, 1 and 4 are carried out for all cross sections, whereas Group 2 and 3 were performed for a single cross-section geometry. Group 0 is the reference group, in which nominal values are taken for all basic variables, and only addresses the variability of the design model and it was used for estimation of the sample size. Group 1 considers the cross-section dimensions (CS) and the material properties (M) as random variables, while Group 4 adds the initial geometrical imperfection – bow imperfection (IMP) and the residual stresses (RS) as random variables. Groups 2 and 3 cover different combinations of random variables for the sensitivity study defined in STEP 2: (M-E) means that the Young's modulus is considered as a deterministic variable while yield stress and ultimate stress are assumed as random variables; (GIMP2) corresponds to an alternative statistical characterization of the initial geometrical imperfections – see Section 3.3; and (RS2) represents an alternative statistical characterization of the residual stresses – see Section 3.4.

### 2.3. Resistance function

The resistance function is flexural buckling of welded I section columns as given in the revised version of Eurocode 3 (FprEN 1993–1-1) [13]. The buckling resistance of a compressed column, $N_{b,Rd}$, is defined by Eq. (1) - cl. 8.3.1 of FprEN 1993–1-1 [13].

$$N_{b,Rd} = \begin{cases} \dfrac{\chi A f_y}{\gamma_{M1}} \; for\ classes\ 1,2\ and\ 3 \\ \qquad / \\ \dfrac{\chi A_{eff} f_y}{\gamma_{M1}} \; for\ class\ 4 \end{cases} \tag{1}$$

where: $f_y$ indicates the yield strength of the material; $\gamma_{M1}$ is the partial factor for the verification of the buckling resistance of members, which is set to 1.0; $\chi$ is the reduction factor related to the flexural buckling modegiven by Eq. (2), in which the buckling parameter $\phi$ is defined by Eq. (3), and the normalized slenderness $\bar{\lambda}$ is calculated by Eq. (4):

$$\chi = \frac{1}{\phi + \sqrt{\phi^2 - \bar{\lambda}^2}} \leq 1 \tag{2}$$

$$\phi = 0.5\left[1 + \alpha(\bar{\lambda} - 0.2) + \bar{\lambda}^2\right] \tag{3}$$

$$\bar{\lambda} = \sqrt{\frac{A f_y}{N_{cr}}}, for\ class\ 1,2\ and\ 3$$

$$\bar{\lambda} = \sqrt{\frac{A_{eff} f_y}{N_{cr}}}, for\ class\ 4 \tag{4}$$

$A$ is the gross cross-section area, $A_{eff}$ is the effective cross-section area when subject to uniform compression, $N_{cr}$ is the elastic critical force

**Table 1**
Groups of samples.

| | Group | Cross-sectional dimensions (CS) | Material properties (M) | | Initial geometric imperfections (IMP) | | Residual stresses (RS) | Step |
|---|---|---|---|---|---|---|---|---|
| | | | $f_y$ (MPa) | $E$ (MPa) | Minor-axis | Major-axis | | |
| Standard Groups (a) | 0 | Deterministic | Deterministic | Deterministic | Deterministic | | Deterministic | 1, 2*, 3 |
| | 1 (random CS + M) | Normal distribution | Lognormal distribution | Normal distribution | Deterministic | | Deterministic | 2*, 3 |
| | 4 (random CS + M + GIMP+RS) | | | | GIMP - Normal distribution | GIMP2 – Weibull distribution | Normal distribution | 1*, 2*, 3 |
| Sensitivity analysis Groups (b) | 1b (random CS + M-E) | | | Deterministic | Deterministic | | Deterministic | 2 |
| | 2 (random CS + M + GIMP) | | | Normal distribution | GIMP - Normal distribution | GIMP2 – Weibull distribution | Deterministic | 2* |
| | 2b (random CS + M + GIMP2) | | | | GIMP2 – Weibull distribution | | Deterministic | 2* |
| | 3 (random CS + M + RS) | | | | Deterministic | | Normal distribution | 2* |
| | 3b (random CS + M + RS2) | | | | Deterministic | | Normal distribution | 2* |
| | 4b (random CS + M + GIMP2 + RS) | | | | GIMP2 – Weibull distribution | | Normal distribution | 2* |
| | 4c (random CS + M-E + GIMP2 + RS) | | | Deterministic | GIMP2 – Weibull distribution | | Normal distribution | 2 |

1* and 2* are only performed for a single cross section.

related to the relevant flexural buckling mode and $\alpha$ is the imperfection factor, which is selected by choosing the appropriate buckling curve.

For class 4 cross sections, $A_{eff}$ is calculated according to EN 1993–1-5 [35], see Eqs. (5) to (13) in Table 2:

Table 3 shows the buckling curves recommended by FprEN 1993–1-1 [13] for HSS welded I-sections (steel grades S460 up to S700). Table 3 also presents the improved choice of buckling curves that is incorporated in an early amendment [32] to FprEN1993–1-1 [13] which is currently being prepared, aligning the reliability of the design provisions for welded and rolled columns.

**Table 3**
Buckling curve selection for welded HSS columns.

| Cross-section | Limits | Buckling about axis | Buckling curve S460 up to S700 | |
|---|---|---|---|---|
| | | | EN/FprEN 1993–1-1 [2,13] | Amendment [18,32] |
| 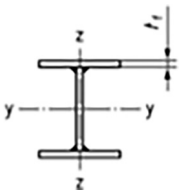 | $t_f \leq 40$ mm | y-y | b | a |
| | | z-z | c | b |
| | $t_f > 40$ mm | y-y | c | b |
| | | z-z | d | c |

### 2.4. Experimental resistance

Using the general-purpose finite element software ABAQUS [36], an advanced finite element (FE) model was used to obtain the ultimate resistance of the pin-ended compressed columns. The FE model is identical to the numerical model created and validated by Ferreira Filho et al. [16], based on the experimental work performed in the project STROBE [15], using welded, doubly symmetric, and homogeneous or hybrid columns and beam-columns.

Geometrically and materially nonlinear analyses including imperfections (GMNIA) were executed, where a compressive load was applied to each generated numerical model according to the Newton-Raphson method used in a force control mode. The overlap between the parts of the cross-sections of the models at the web-flange junctions was prevented and tie constraints were applied at these regions to guarantee the appropriate connection. Fig. 1 shows an example of the base geometry of the numerical model, illustrating the main geometrical parameters. Without loss of accuracy, it is noted that the longitudinal welds between the web and the flanges were not modelled because their impact on the reliability assessment is negligible since the code assessment was also carried out with a cross-sectional area that disregarded those welds. Nevertheless, a verification study was carried out that has shown that the beneficial influence of the welds on the resistance of the columns is of the order of 2%.

The material model was adopted according to Yun and Gardner [37] as a true stress-strain curve exhibited in Fig. 2.

The columns were modelled with shell elements using four-node finite element with full integration S4 from the ABAQUS library [36]. From a mesh sensitivity study, a mesh composed of 16 elements across the flanges' width and other 16 across the web's depth was adopted. The length of the elements was chosen such that the finite elements were approximately square.

All columns were simply supported at both ends. Following guidance from Braun et al. [38], the restrictions to lateral and vertical displacements were applied at the nodes coincident with the centroids of each end-section, as well as the restrictions to torsional rotation. The restricted nodes were set as master nodes, in which all the other nodes of the end-sections were coupled. In this sense, the end-sections remained plane along the entire load application process. In addition, only for major-axis buckling, the out-of-plane displacements were prevented along the length of the flanges and web to force in-plane displacements in all cross-sections of the members. The axial compressive force was concentrically applied at one of the master nodes, while the longitudinal displacement was prevented at the other.

Regarding the imperfections, the membrane residual stresses were introduced at partitions done in the web and flange parts of the model by defining the initial stresses through the predefined field command within ABAQUS [36] and the initial geometric imperfections with the shape of a half-wave sine function were automatically introduced into each node of the numerical model by a MATLAB subroutine. Finally, the GMNIA analyses were executed to obtain the ultimate load of each numerical model generated.

### 2.5. Parametric study

The parametric study consisted of the following welded sections (Table 4). These sections cover the various cross-sectional geometries that are typical of equivalent rolled profiles, as well as deeper I-girders typically used in bridge construction. All cross sections were analysed for minor- and major-axis flexural buckling. Table 4 also reports the

**Table 2**
Effective area for class 4 sections.

$$A_{eff} = \rho_f A_f + \rho_w A_w \quad (5)$$

Flanges

$$\begin{cases} \rho_f = 1.0 \text{ for } \bar{\lambda}_p \leq 0.748 \\ \rho_f = \dfrac{\bar{\lambda}_p - 0.188}{\bar{\lambda}_p^2} \text{ for } \bar{\lambda}_p > 0.748 \end{cases} \quad (6a)$$

$$\bar{\lambda}_p = \frac{c_f/t_f}{12.212\,\epsilon} \quad (7a)$$

$$\epsilon = \sqrt{\frac{235}{f_y}} \quad (8)$$

$$c_f = \frac{b}{2} - 1.5t_w \quad (9a)$$

Web

$$\begin{cases} \rho_w = 1.0 \text{ for } \bar{\bar{\lambda}}_p \leq 0.673 \\ \rho_w = \dfrac{\bar{\lambda}_p - 0.22}{\bar{\lambda}_p^2} \text{ for } \bar{\lambda}_p > 0.673 \end{cases} \quad (6b)$$

$$\bar{\bar{\lambda}}_p = \frac{c_w/t_w}{113.6\,\epsilon} \quad (7b)$$

$$c_w = d - 2t_w \quad (9b)$$

where: $A_f$ and $A_w$ are the gross area of the flanges and web, respectively; $\rho_f$ and $\rho_w$ are the reduction factors for plate buckling related to the flanges and web, respectively, and calculated by Eq. (6a) and (6b); $\bar{\lambda}_p$ is the slenderness of the plates given by Eq. (7a) and (7b); $c_f$ and $c_w$ are the appropriate widths of the flange and web plates, respectively, which is given in Eq. (9a) and (9b); $t_f$ and $t_w$ are the thicknesses of the flange and web, respectively; $b$ and $d$ are the flange width and web depth, respectively.

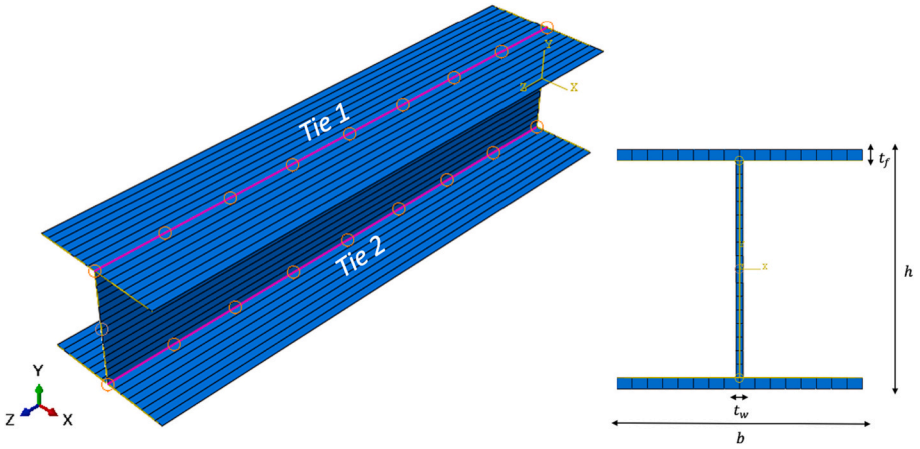


**Fig. 1.** Example of the reference geometry of the numerical models.

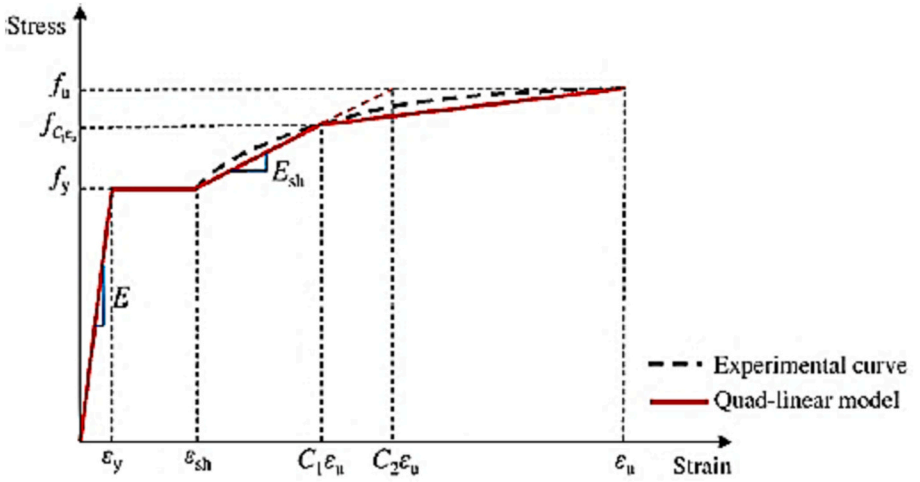


**Fig. 2.** Quad-linear model representing the true stress-strain curve proposed by Yun and Gardner [37].

**Table 4**
Definition of selected cross sections for parametric study.

| Cross-section | Equivalent cross-section | Cross-section class | | Normalized slenderness $\bar{\lambda}$ | n | Buckling mode |
|---|---|---|---|---|---|---|
| | | Flanges | Web | 6 | 290,126 | |
| HE300A | HEA 300 eq. | 4 | 4 | 0.3; 0.6; 1.0; 1.4; 1.8; 2.2 | 90,030 | In Plane (y-y) |
| IPE160 | IPE 160 eq. | 2 | 4 | | 48,024 | Out Plane (z-z) |
| | | | | | 32,020 | |
| HL1100 | HLM 1100 eq. | 1 | 4 | | 32,020 | |
| HL1500 | HLM 1500 eq. | 1 | 4 | | 68,022 | |
| HE280M | HEM 280 eq. | 1 | 1 | | 20,010 | |
| HD400 | HD 400 × 1299 | 1 | 1 | | | |

number of FEM analyses that totalled 146,000 for the Sensitivity Groups and 144,126 for the Standard Groups (92,100 for minor-axis and 52,026 for major-axis buckling). The total number of FEM analyses (290126) took 9 months to run in a fast Workstation with 12 Intel cores.

## 3. Statistical data

### 3.1. Geometrical properties

The geometrical properties were stochastically defined for all the samples generated to carry out the reliability assessment. The statistical parameters from table E.2 of Annex E of FprEN1993–1-1 [13] were adopted for the cross-sectional dimensions using a Gaussian distribution with the nominal, mean and c.o.v. values specified in Table 5.

### 3.2. Material properties

The high-strength steel grade covered herein is S690. Yield strength, $f_y$, modulus of elasticity, $E$, and ultimate strength, $f_u$, were considered as random variables. The statistical parameters were extracted from table E.1 of Annex E of FprEN1993–1-1 [13], which reflects the current European steel production. The statistical values of the yield and ultimate strength were described by a lognormal distribution. A Gaussian distribution was adopted for the modulus of elasticity. The nominal, mean and c.o.v. values for both variables are shown in Table 6.

**Table 5**
Statistical parameters of the geometric properties.

| Cross-sections | Nominal (mm) | | | | Mean (mm) | | | | c.o.v. (%) | | | |
|---|---|---|---|---|---|---|---|---|---|---|---|---|
| | h | $b_f$ | $t_f$ | $t_w$ | h | $b_f$ | $t_f$ | $t_w$ | h | $b_f$ | $t_f$ | $t_w$ |
| HE300A | 290 | 300 | 14 | 8.5 | 290 | 300 | 13.7 | 8.5 | 0.9 | 0.9 | 2.5 | 2.5 |
| HE280M | 310 | 288 | 33 | 18.5 | 310 | 288 | 32.3 | 18.5 | | | | |
| HL1100 | 1108 | 402 | 40 | 22 | 1108 | 402 | 39.2 | 22 | | | | |
| HL1500 | 1500 | 402 | 40 | 22 | 1500 | 402 | 39.2 | 22 | | | | |
| IPE160 | 160 | 82 | 7.2 | 5 | 160 | 82 | 7.05 | 5 | | | | |
| HD400 | 600 | 476 | 140 | 100 | 600 | 476 | 137.2 | 100 | | | | |

**Table 6**
- Statistical parameters of the material properties [13].

| S690 | $f_y$ | $f_u$ | $E$ |
|---|---|---|---|
| Nominal (MPa) | 690 | 855 | 210,000 |
| Mean (MPa) | 759 | 940.5 | 200,000 |
| c.o.v (%) | 3.5 | 3.5 | 3.0 |

### 3.3. Initial geometrical imperfections

The initial geometric imperfections can be defined according to two parameters: shape and amplitude. As a conservative estimate, the lowest global modes obtained by previous modal analyses, which have the shape of a half-wave sine function, are generally applied as the imperfection shape for parametric studies available in the literature [10,39–41]. The same was also done herein, always employing this deterministic imperfection shape.

Concerning the amplitude, three possibilities were considered (Table 7): a deterministic amplitude equal to $e_0 = L/1000$, [42]; GIMP - a Gaussian distribution with the mean and c.o.v. values determined from a data collection performed on measurements for high-strength steel welded I-section columns available in recent studies in the literature [21–31], only for minor-axis; or GIMP2 - a random amplitude following the Weibull distribution with the statistical properties proposed by Fukumoto and Itoh [43]. As the recent measurements related to the major-axis of HSS members are scarce in the literature, the statistical characterization proposed by Fukumoto and Itoh [43] was adopted for all cases with respect to the initial geometric imperfections related to the major-axis.

### 3.4. Residual stresses

The residual stress pattern was considered as deterministic for all groups according to the model proposed by Schaper et al. [20], illustrated in Fig. 3, which was validated against an extensive data of residual stress measurements with steel grades from S235 to S890, considering both the cross-section geometry and steel grade in the formulation, and provided a better representation of residual stresses when compared to the models of ECCS [42] and prEN1993–1-14 [44], especially for HSS members.

Regarding the magnitudes, three possibilities were considered: (a) deterministic magnitudes in accordance with the Schaper et al. model [20]; (b) RS - random magnitudes following a Gaussian distribution with the statistical parameters extracted from Tankova et al. [19]; and (c) RS2 - statistical parameters for the Gaussian distribution obtained from the most recent measurements available in the literature for HSS welded I-section members [45–53]. For RS, Table 8 shows the statistical parameters for the compression residual stresses of the flanges, $\sigma_{f,c}$, and the web, $\sigma_{f,w}$, the tensile residual stresses being found by equilibrium. For RS2, Table 9 presents the statistical parameters for the residual stresses in the web and flanges.

**Table 7**
Statistical parameters of the amplitude of the initial geometrical bow imperfections.

| | GIMP: data collection for HSS | GIMP2: Fukumoto and Itoh [43] | |
|---|---|---|---|
| Buckling type | Minor-axis $e_0/L$ | Major-axis $e_0/L$ | Minor-axis $e_0/L$ |
| Mean | 0.000585 | 0.000125 | 0.000296 |
| c.o.v (%) | 54 | 92 | 81 |
| n | 64 | 68 | |

## 4. Monte Carlo simulation: initial benchmarks, sensitivity studies and statistical assessment

### 4.1. Initial benchmarks

A set of initial benchmarks was carried out to ensure that the Monte Carlo simulation would lead to reliable results and to assess the influence of some phenomena that could affect the reliability assessment of the flexural buckling resistance of columns. They are addressed in the following sub-sections.

#### 4.1.1. Sample size

The Monte Carlo simulation starts with the generation of random numbers for the selected random variables with prescribed probabilistic distributions [34]. As the accuracy of the solutions obtained through Monte Carlo simulations improves with sample size, it is desirable to have as large number as possible. On the other hand, this number should be minimized because of the computation time. Hence, sample sizes of 333, 1000 and 2000 columns were considered per slenderness for Group 4 with cross section HE 280 M, slenderness between 0.3 and 2.2, and minor axis buckling, totaling 19,998 numerical models. Table 10 shows the statistical parameters for all slenderness ranges for the three sample sizes and Fig. 4 to Fig. 6 illustrate normal probability plots for the three sample sizes per slenderness. The statistical parameters are presented as normalized to the nominal column resistance, hence values higher than 1.0 indicate that the simulation is safe-sided, and values lower than 1.0 unsafe sided. In Table 10, it is possible to see the number of cases with values lower than one and they are used to calculate the probability of the buckling resistance being lower than the cross-section resistance. This probability is denoted as "*pf**" in Table 10 and it is given as the ratio between the number of cases lower than one and the total number. The statistical parameters for sample sizes of 1000 and 2000 are very close, therefore it was considered that a sample size of 1000 can be assumed.

Furthermore, it is noted that for slenderness ratios 1.0 and 1.4, there are no cases which fall on the unsafe side, which can be considered as an indicator that a larger sample size is required. Yet, when the probability plots in Fig. 5 and Fig. 6 are observed, it is seen that extrapolating the curves of for slenderness 1.0 and 1.4, the results will lead to a probability which is much lower than the 0.00118 quantile (the corresponding quantile of the resistance to define the appropriate design values, $r_d$ – see Subsection 5.1), and therefore, the sample size is kept at 1000.

Additionally, the distribution of the data obtained with the population of 1000 samples was verified by the Chi-square distribution test,

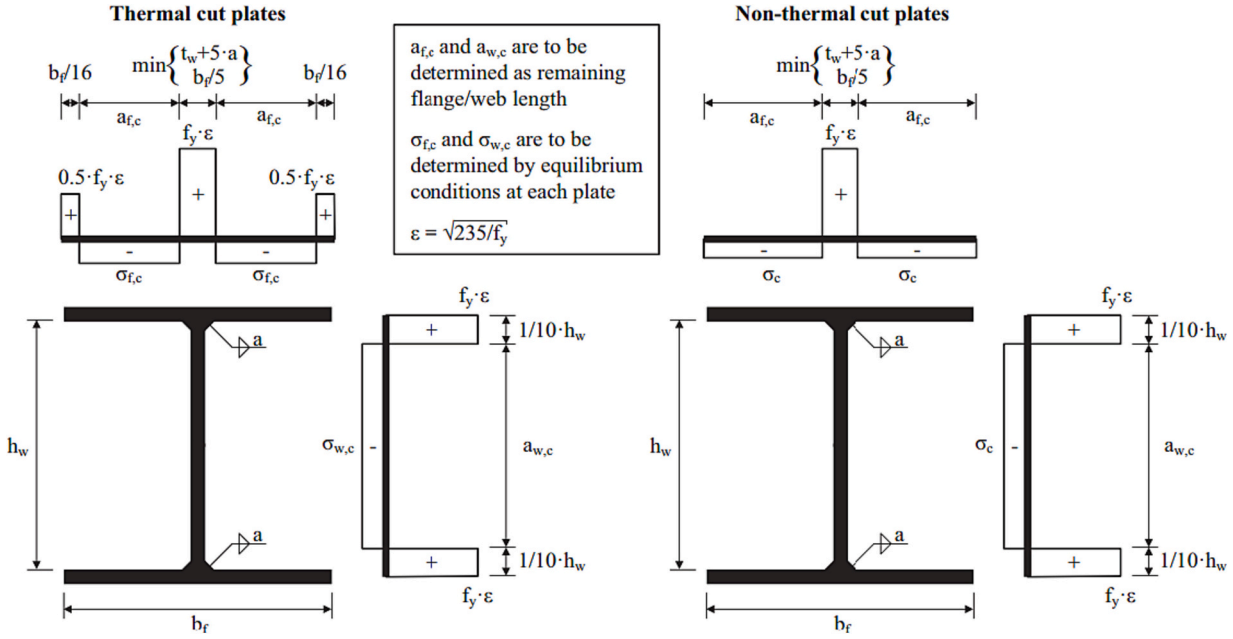


**Fig. 3.** Novel model for residual stresses of welded I-section columns made with thermal cut plates [15].

**Table 8**
Statistical parameters of the magnitude of compressive residual stresses.

| | $\sigma_{f,c}$ | $\sigma_{w,c}$ |
|---|---|---|
| Mean (MPa) | $-0.13f_y = -89.7$ | $-0.13f_y = -89.7$ |
| c.o.v. (%) | 43 | 38 |

**Table 9**
Statistical parameters of the magnitudes of residual stresses based on the data collection for S690 HSS welded I-section columns.

| | Flange compression $\sigma_{f,c}$ | Flange tension $\sigma_{f,t}$ | Web compression $\sigma_{w,c}$ | Web tension $\sigma_{w,t}$ |
|---|---|---|---|---|
| Mean (MPa) | −112.3 | 363.6 | −79.1 | 227.4 |
| c.o.v. (%) | −29.03 | 43.20 | −48.39 | 44.89 |
| n | 18 | 18 | 18 | 17 |

also called "goodness-of-fit", with 1% significance level [40,54]. The assumption of a Gaussian distribution in all slenderness cases was accepted by the test, concluding that the ultimate resistance results from the Monte Carlo simulations can be considered as normally distributed for the slenderness range considered.

*4.1.2. Local buckling*

Class 4 cross sections may exhibit an additional reduction of the buckling resistance due to local buckling. This effect is more pronounced for HSS, as shown in Table 4, which shows that four (out of six) of the selected cross sections are class 4.

Since it is not the aim of this paper to assess the reliability of the reduction factors for local instability, it was necessary to define a strategy on how to split these two phenomena. Firstly, the strategy to compare the results of the advanced FE simulations and the Eurocode buckling resistance was defined as follows:

- to use Group 0, for minor-axis only;
- to compare the numerical (FEM) and EC3 buckling resistances considering local buckling of the whole cross-section (C1), considering the following two cases:

**Table 10**
Statistical parameters for the various sample sizes.

| $n = 333$ | | | | | | |
|---|---|---|---|---|---|---|
| Slenderness | 0.3 | 0.6 | 1 | 1.4 | 1.8 | 2.2 |
| **mean** | 1.114 | 1.163 | 1.393 | 1.385 | 1.312 | 1.270 |
| **stdev** | 0.047 | 0.059 | 0.093 | 0.090 | 0.083 | 0.079 |
| **cov** | 4.19% | 5.07% | 6.65% | 6.52% | 6.34% | 6.23% |
| **min** | 0.990 | 1.027 | 1.150 | 1.175 | 1.093 | 1.053 |
| **<1** | 3 | 0 | 0 | 0 | 0 | 0 |
| **pf*** | 0.009 | 0 | 0 | 0 | 0 | 0 |
| ***n* = 1000** | | | | | | |
| **Slenderness** | **0.3** | **0.6** | **1** | **1.4** | **1.8** | **2.2** |
| **mean** | 1.106 | 1.148 | 1.293 | 1.181 | 1.108 | 1.073 |
| **stdev** | 0.050 | 0.062 | 0.082 | 0.062 | 0.054 | 0.051 |
| **cov** | 4.48% | 5.38% | 6.36% | 5.21% | 4.92% | 4.77% |
| **min** | 0.973 | 0.952 | 1.073 | 1.014 | 0.940 | 0.901 |
| **<1** | 12 | 4 | 0 | 0 | 17 | 77 |
| **pf*** | 0.012 | 0.004 | 0 | 0 | 0.017 | 0.077 |
| ***n* = 2000** | | | | | | |
| **Slenderness** | **0.3** | **0.6** | **1** | **1.4** | **1.8** | **2.2** |
| **mean** | 1.100 | 1.145 | 1.286 | 1.178 | 1.104 | 1.069 |
| **stdev** | 0.049 | 0.063 | 0.087 | 0.062 | 0.053 | 0.051 |
| **cov** | 4.43% | 5.46% | 6.76% | 5.23% | 4.82% | 4.74% |
| **min** | 0.966 | 0.958 | 1.051 | 1.009 | 0.955 | 0.922 |
| **<1** | 27 | 9 | 0 | 0 | 40 | 161 |
| **pf*** | 0.014 | 0.0045 | 0 | 0 | 0.020 | 0.0805 |

- C1.FEM - Group 0 without any cross-section restraints to prevent local buckling calculated using FEM;
- C1.EC3 - Group 0 calculated using Eurocode 3 considering local buckling.
- to compare the numerical (FEM) and EC3 buckling resistances considering local buckling only in the web (C2), considering the following two cases:
- C2.FEM - Group 0 with the vertical displacement prevented at the tips of the flanges to prevent their local buckling, calculated using FEM;
- C2.EC3 - Group 0 calculated using Eurocode 3 neglecting local buckling in the flanges.

These two cases, C1 and C2, were considered because among all class 4 cross-sections, a large proportion results from the slenderness of the

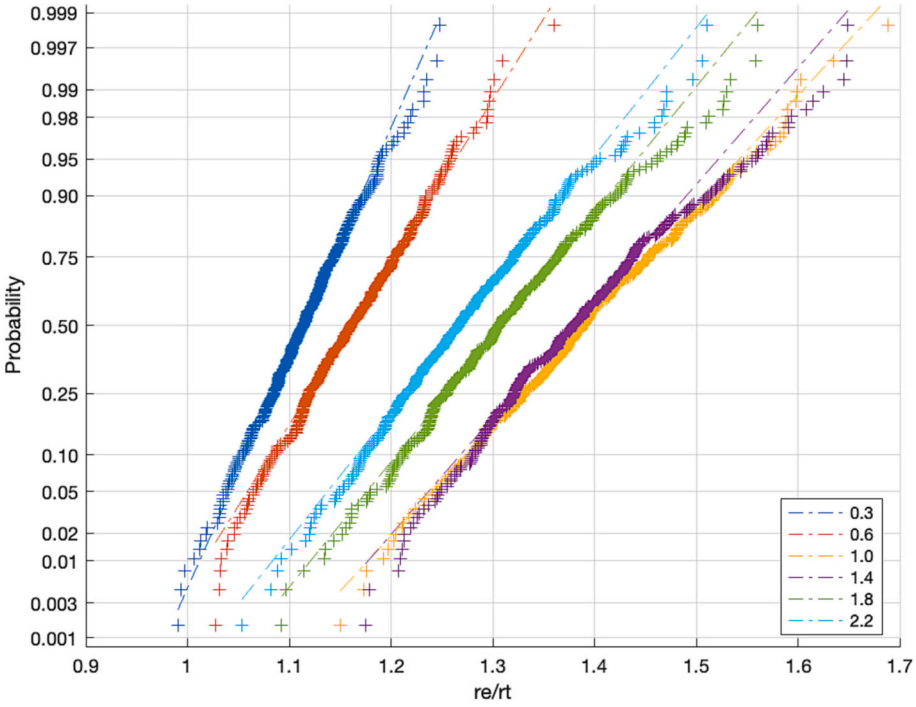


**Fig. 4.** Normal probability plot with sample size equal to 333.

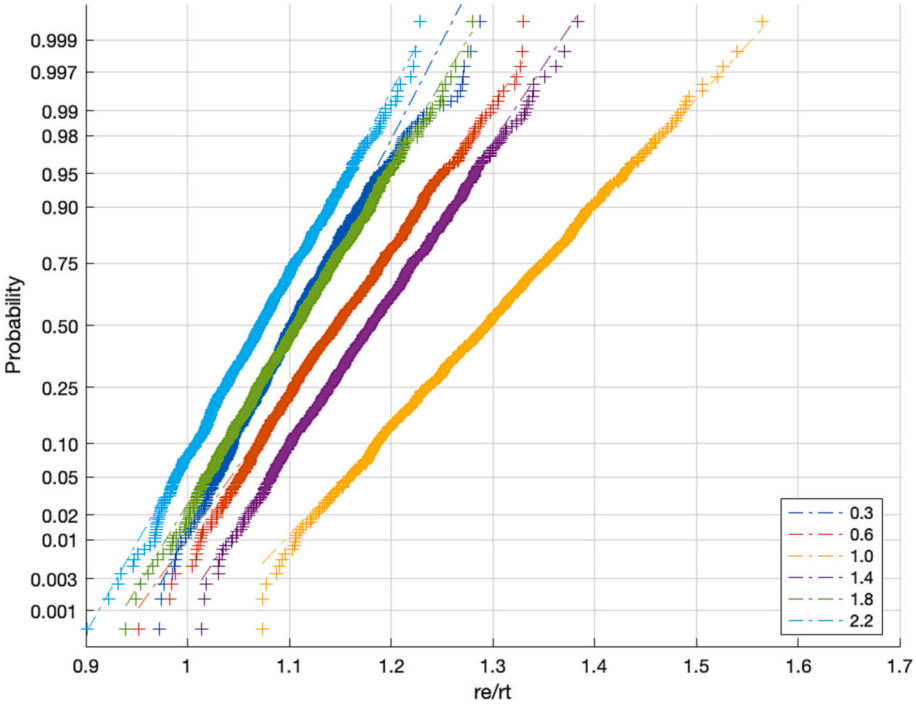


**Fig. 5.** Normal probability plot with sample size equal to 1000.

web, as seen in Table 4. The results show that for all cross sections, the maximum difference between the numerical and the EC3 results occurs mostly for the low slenderness range and reduces as the global slenderness increases. Fig. 7 shows the variation of the average ratio $r_{FEM}/r_{EC3}$ with slenderness for both cases and the six slenderness ranges.

Except for the HE 300 A cross section in the low slenderness range ($\leq$ 0.6) that exhibits class 4 flanges, the difference between the average ratios $r_{FEM}/r_{EC3}$ for C1 and C2 is small (1.15 vs 1.16, respectively). Henceforth, for minor-axis buckling, the numerical models were implemented with the vertical displacement prevented at the tips of the flanges and always compared with the resistance calculated according to EC3 neglecting local buckling in the flanges.

Secondly, as the numerical models assumed a global out-of-plane initial bow imperfection as described in Section 4.3, it was further investigated whether different combinations of initial imperfections (global and local) could lead to lower buckling resistances. Hence, the results from GMNIA analyses for Group 0 with different types of initial imperfection shapes: (a) Global buckling eigenmode; (b) Local buckling

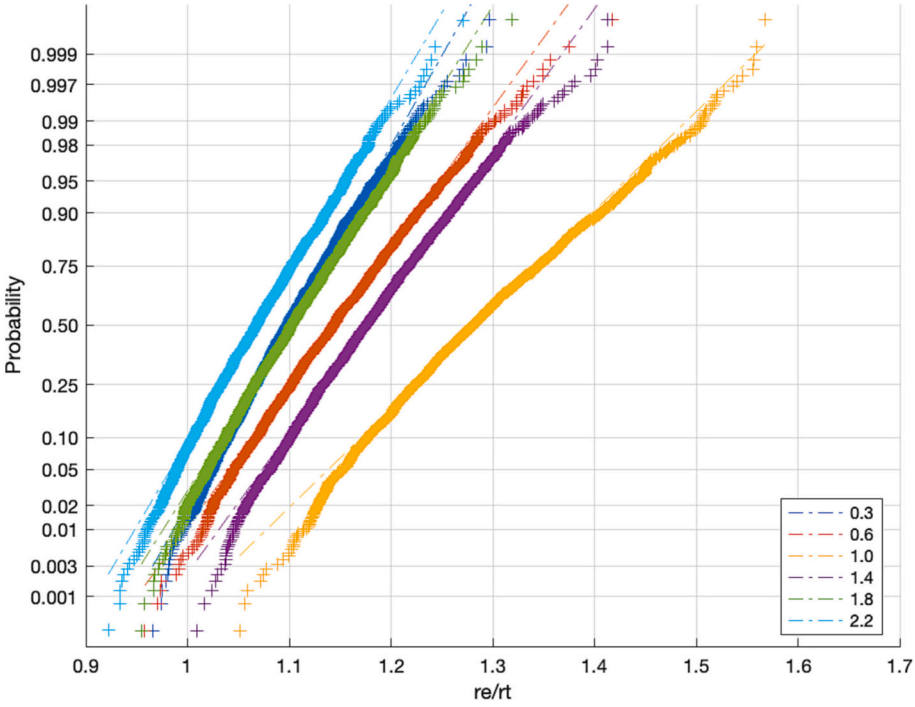


**Fig. 6.** Normal probability plot with sample size equal to 2000.

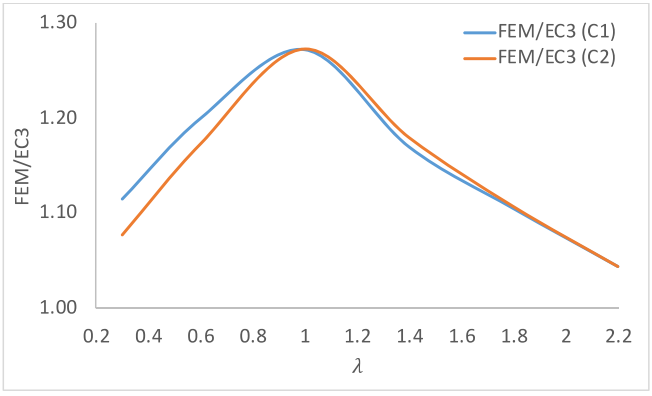


**Fig. 7.** Average ratios $r_{FEM}/r_{EC3}$.

eigenmode; (c) Global-70Local buckling eigenmode - combined global and local modes with the global mode as the leading imperfection; (d) Local-70Global buckling eigenmode - combined local and global modes with the local mode as the leading imperfection. The variation of the average reduction factor, $\chi_{FEM}$, with slenderness for all sections is plotted in Fig. 8.

The global imperfection led to the lowest result for the majority of the cases. For the Class 1-sections, it was the critical initial imperfection for all sections and slendernesses. For the Class 4-sections, the global imperfection always led to the lowest values for the intermediate and slender columns ($\lambda = 1.0$ *to* 2.2). However, for slenderness, $\lambda$, equal to 0.3, the local imperfection was critical, leading to an average buckling resistance 3.3% lower than the global imperfection. For $\lambda = 0.6$, this trend was maintained only for cross-sections IPE160 and HL1500, with average values 3.4% lower.

Since a global initial imperfection was critical for almost all members analysed and, in the cases where local initial imperfections were critical, the differences were <3.5%, a global initial imperfection was adopted in the parametric study for pragmatic reasons related to the time required to carry out the parametric study.

#### 4.1.3. *Influence of the cutting process*

Finally, a third initial benchmark considered the influence of using non-thermal cut plates and their influence on the residual stresses. Group 0 was selected for this benchmark, for minor-axis only, comparing the following cases: (i) Group 0 with the residual stress pattern for thermal cut plates and (ii) Group 0 with the residual stress pattern for non-thermal cut plates (Fig. 3). The average difference for all cases was 1.01 so the pattern for thermal cut plates was chosen (Table 11).

### 4.2. *Sensitivity studies*

The sensitivity studies were performed for a single cross section, HEA 300 eq., and minor-axis buckling to reduce the global sample size, as shown in Table 1. The buckling resistance related to minor-axis flexural buckling was extracted from each FEM simulation to statistically characterize the resistance predicted by each group. It originated Probability Density Functions (PDFs) for each group, which were well described by Gaussian distributions.

#### 4.2.1. *Influence of the number of basic random variables*

The influence of the number of basic random variables is assessed by comparing the results of groups 1 (CS + M), 2 (CS + M + GIMP), 3 (CS + M + RS) and 4 (CS + M + GIMP+RS), all normalized with respect to the results of Group 0 (no random variables). Table 12 shows that there is a negligible influence of the consideration of the material properties and the cross-section geometry as random variables (1.4%) because the overstrength of steel compensates for the other properties. The comparison of Group 2 with Group 0 shows that there is a beneficial effect of considering the initial geometrical imperfections as random (1.4%), while the comparison of Group 3 with Group 0 highlights a neutral (but on the safe side) effect of random residual stresses (1.3%). Finally, comparing Group 4 with Group 0 shows that it is safe to consider only the variability of the design model (2.1%).

Fig. 9 depicts the normalized resistance and the corresponding statistical descriptors, split according to slenderness ranges. All cases show larger ratios of flexural resistance when compared to Group 0 in the

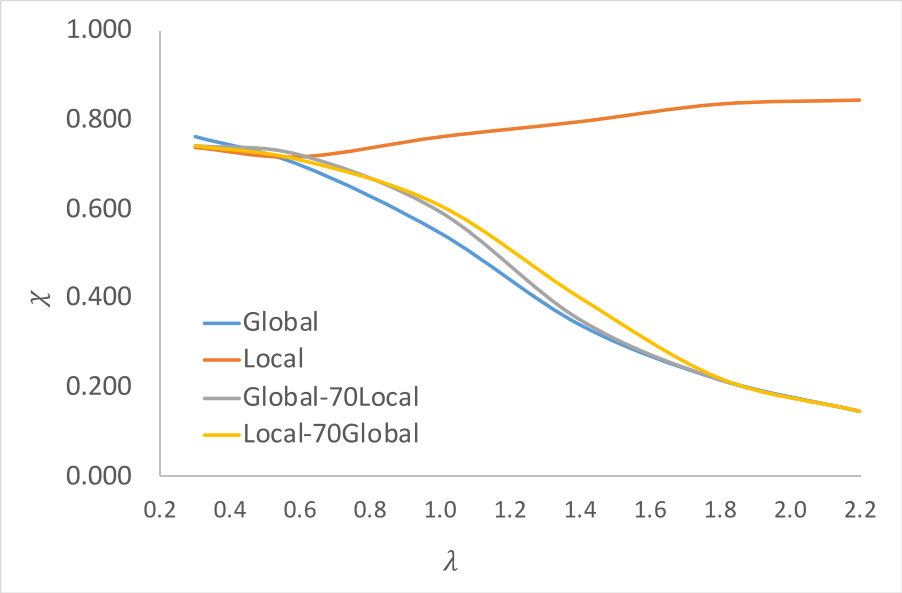


**Fig. 8.** Average numerical reduction factors from different types of initial imperfections.

**Table 11**
Comparison between residual stress pattern for thermal cut plates and non-thermal cut plates.

| SECTION | Class | λ | Thermal cut | Non-thermal cut | Dif. |
|---|---|---|---|---|---|
| HE 300 A | 4 | 0.3 | 0.974 | 0.964 | 1.01 |
| | | 0.6 | 0.879 | 0.874 | 1.01 |
| | | 1.0 | 0.679 | 0.682 | 1.00 |
| | | 1.4 | 0.425 | 0.423 | 1.00 |
| | | 1.8 | 0.277 | 0.276 | 1.00 |
| | | 2.2 | 0.181 | 0.18 | 1.01 |
| IPE 160 | | 0.3 | 0.978 | 0.967 | 1.01 |
| | | 0.6 | 0.883 | 0.873 | 1.01 |
| | | 1.0 | 0.669 | 0.671 | 1.00 |
| | | 1.4 | 0.421 | 0.419 | 1.00 |
| | | 1.8 | 0.262 | 0.26 | 1.01 |
| | | 2.2 | 0.182 | 0.181 | 1.01 |
| HE 280 M | 1 | 0.3 | 0.977 | 0.964 | 1.01 |
| | | 0.6 | 0.876 | 0.872 | 1.00 |
| | | 1.0 | 0.671 | 0.675 | 0.99 |
| | | 1.4 | 0.405 | 0.403 | 1.00 |
| | | 1.8 | 0.261 | 0.26 | 1.00 |
| | | 2.2 | 0.180 | 0.179 | 1.01 |
| HL 1100 M | 4 | 0.3 | 0.865 | 0.905 | 0.96 |
| | | 0.6 | 0.812 | 0.814 | 1.00 |
| | | 1.0 | 0.650 | 0.651 | 1.00 |
| | | 1.4 | 0.384 | 0.381 | 1.01 |
| | | 1.8 | 0.245 | 0.244 | 1.00 |
| | | 2.2 | 0.163 | 0.162 | 1.01 |
| HL 1500 M | | 0.3 | 0.785 | 0.781 | 1.01 |
| | | 0.6 | 0.746 | 0.737 | 1.01 |
| | | 1.0 | 0.611 | 0.548 | 1.11 |
| | | 1.4 | 0.406 | 0.404 | 1.00 |
| | | 1.8 | 0.255 | 0.253 | 1.01 |
| | | 2.2 | 0.167 | 0.166 | 1.01 |
| | | | | Mean: | 1.01 |

intermediate slenderness range and increasing scatter with slenderness.

#### 4.2.2. Effects of the modulus of elasticity

The modulus of elasticity is prescribed in EN 1993–1-1 as 210 GPa. In addition, there is no standard testing procedure for its determination. Hence, part of its scatter can be attributed to the measurement procedure and thus its consideration as a random variable is questionable. Hence, the effect of modulus of elasticity as a random variable was assessed for groups 1 and 1b and 4b and 4c (Table 1). Considering all sections and slenderness, when $E$ was considered deterministic, the resistance was improved up to 4.5% and 2.7% on average, respectively, for minor- and major-axis flexural buckling.

Fig. 10 compares both sets of groups with results from all sections and slenderness showing, as expected, that Young's modulus mostly influences the results for the large slenderness range (4.5% to 9%). Also, its influence is similar comparing Groups 1 and 4, mostly for major-axis flexural buckling.

#### 4.2.3. Sensitivity to imperfections

The sensitivity to the statistical characterization of the geometrical and material imperfections was studied by considering groups 2 and 2b, 3 and 3b and 4 and 4b. Fig. 11a compares the results of groups 2 and 2b and 4 and 4b, showing that the measurements from Fukumoto and Itoh [43] yield a beneficial effect that reaches 6.28% for the intermediate slenderness range while the c.o.v. is similar for both groups, increasing from 1% to 5.5% from low to medium/high slenderness. Fig. 11b compares the results of groups 3 and 3b, showing a negligible difference between both groups (<1.4%) and similar c.o.v. for both groups, below 5% for all slenderness ranges.

### 4.3. Statistical assessment

*Groups 0, 1 ($CS \pm M$)* and *4 ($CS \pm M \pm GIMP \pm RS$)*, were selected to statistically characterize the buckling resistance of welded columns. 1000 MC simulations for each slenderness of each cross-section, considering both groups, were carried out, totaling 144,126 analyses to assess the minor- and major-axis flexural buckling resistance of compressive members. From each simulation, the normalized buckling resistance was computed (normalized concerning the nominal cross section resistance) and used to create resistance Probability Distributed Functions (PDFs) for each slenderness and each group. The statistical parameters from groups 1 and 4 were normalized with respect to the results of group 0 and they are exhibited in Table 13 and Table 14 for minor- and major-axis flexural buckling, respectively. Additionally, the results obtained using the Eurocode 3 design expressions are also assessed, disregarding local buckling of the flanges, as described in Section 5.1.

Comparing first the mean values of resistance for all cases, Table 13 and Table 14 show that all results from group 0 are always higher than the results given by EC3 (11% and 9%, on average, for minor- and major-

**Table 12**
Statistical parameters of the reduction factors, $\chi$, for the various groups for HEA 300 and minor-axis flexural buckling.

| FB | | Group 0 | Group 1 (CS + M) | Group 2 (CS + M + GIMP) | Group 3 (CS + M + RS) | Group 4 (CS + M + GIMP + RS) |
|---|---|---|---|---|---|---|
| $\lambda = \mathbf{0.3}$ | Mean | 0.974 | 0.999 | 1.009 | 0.994 | 1.004 |
| | c.o.v. (%) | | 0.423 | 1.006 | 0.602 | 1.286 |
| $\lambda = \mathbf{0.6}$ | Mean | 0.879 | 0.995 | 1.009 | 0.999 | 1.029 |
| | c.o.v. (%) | | 0.318 | 1.544 | 2.927 | 3.475 |
| $\lambda = \mathbf{1.0}$ | Mean | 0.679 | 0.998 | 1.062 | 1.007 | 1.078 |
| | c.o.v. (%) | | 2.270 | 5.171 | 3.829 | 5.514 |
| $\lambda = \mathbf{1.4}$ | Mean | 0.425 | 0.980 | 1.021 | 0.982 | 1.027 |
| | c.o.v. (%) | | 4.255 | 5.568 | 4.367 | 5.001 |
| $\lambda = \mathbf{1.8}$ | Mean | 0.277 | 0.950 | 0.975 | 0.950 | 0.977 |
| | c.o.v. (%) | | 4.618 | 5.318 | 4.715 | 5.075 |
| $\lambda = \mathbf{2.2}$ | Mean | 0.181 | 0.992 | 1.010 | 0.991 | 1.012 |
| | c.o.v. (%) | | 4.668 | 5.232 | 4.857 | 5.016 |
| **ALL** | **Mean** | | 0.986 | 1.014 | 0.987 | 1.021 |
| | **c.o.v. (%)** | | 2.759 | 3.973 | 3.550 | 4.228 |

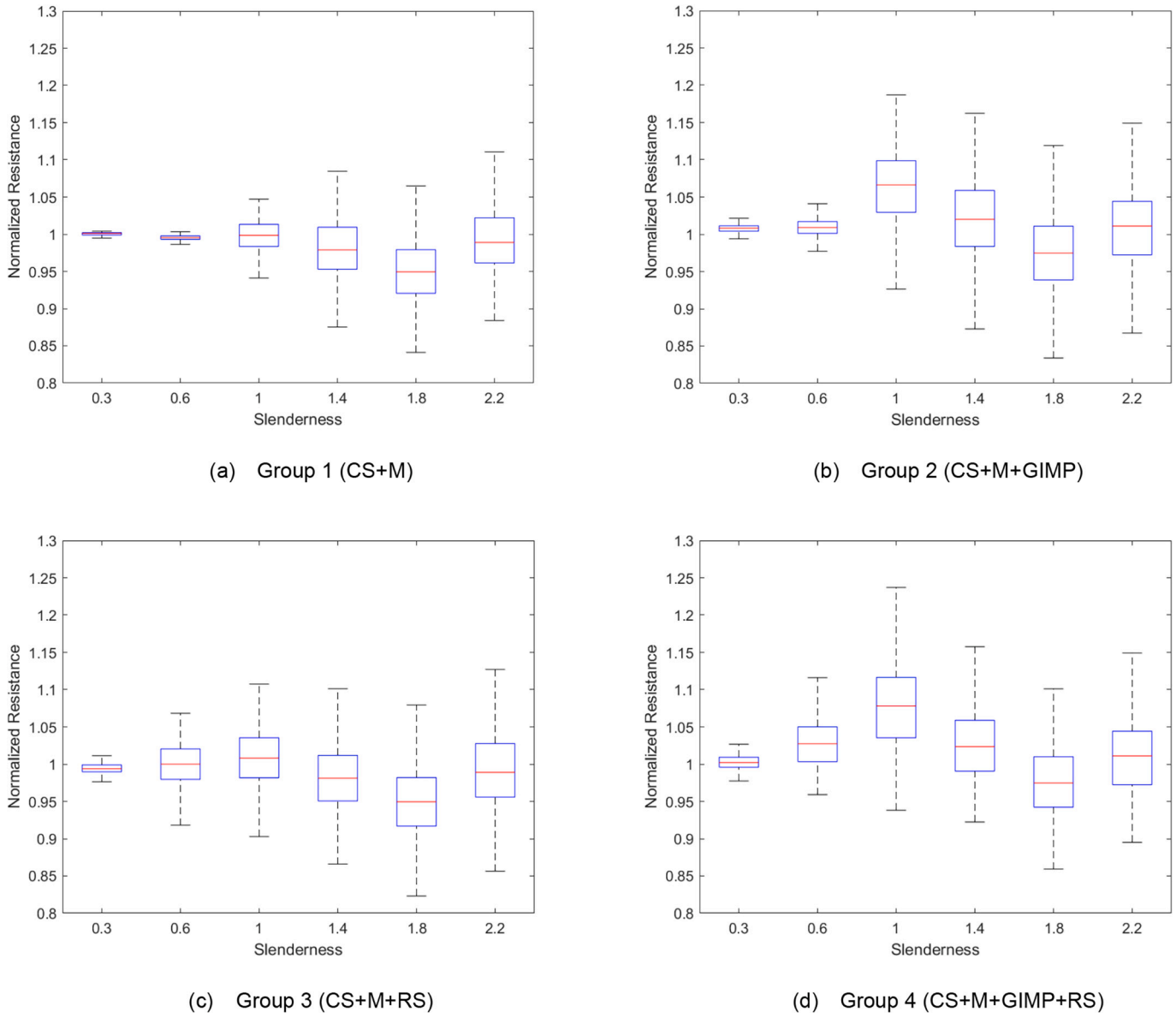


**Fig. 9.** Normalized resistance results for the main groups of analysis considering minor-axis flexural buckling of HEA 300-section columns.

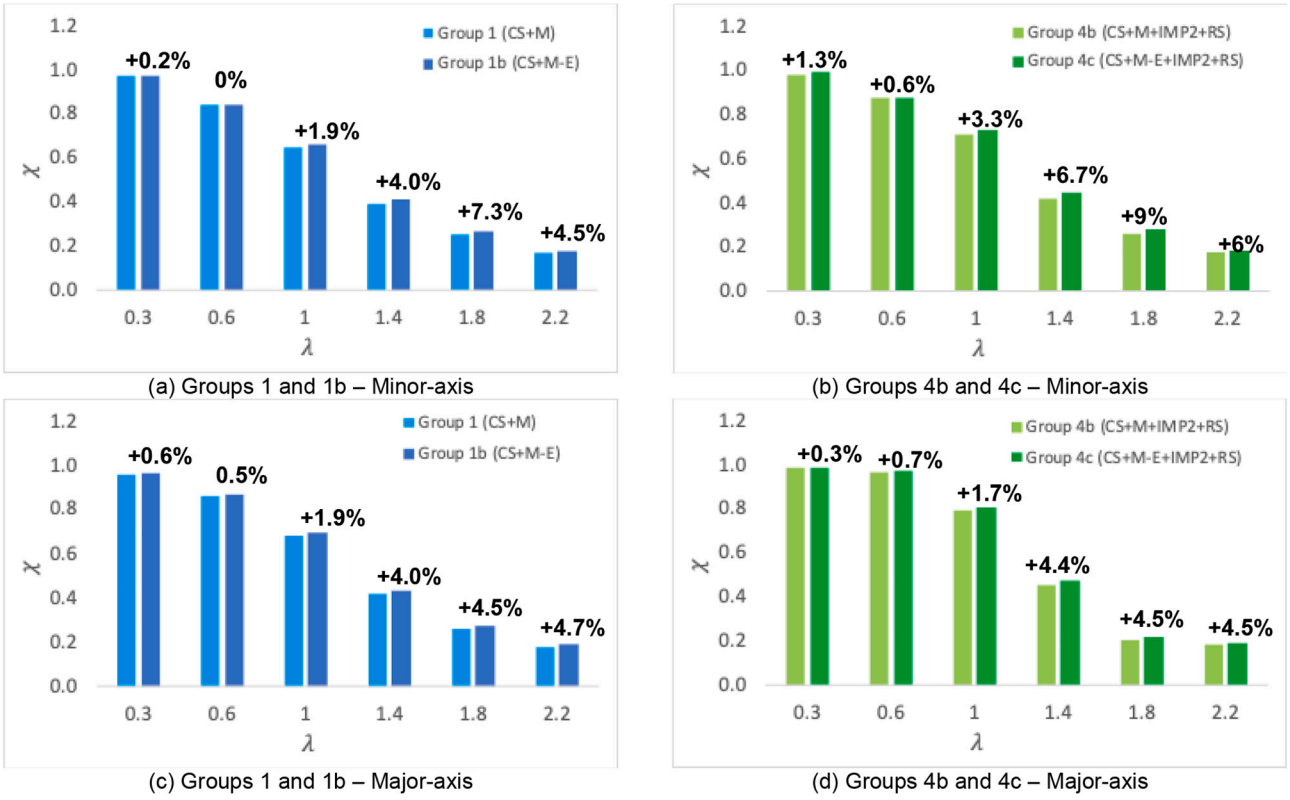


**Fig. 10.** Effects of the randomness of the modulus of elasticity on the buckling resistance.

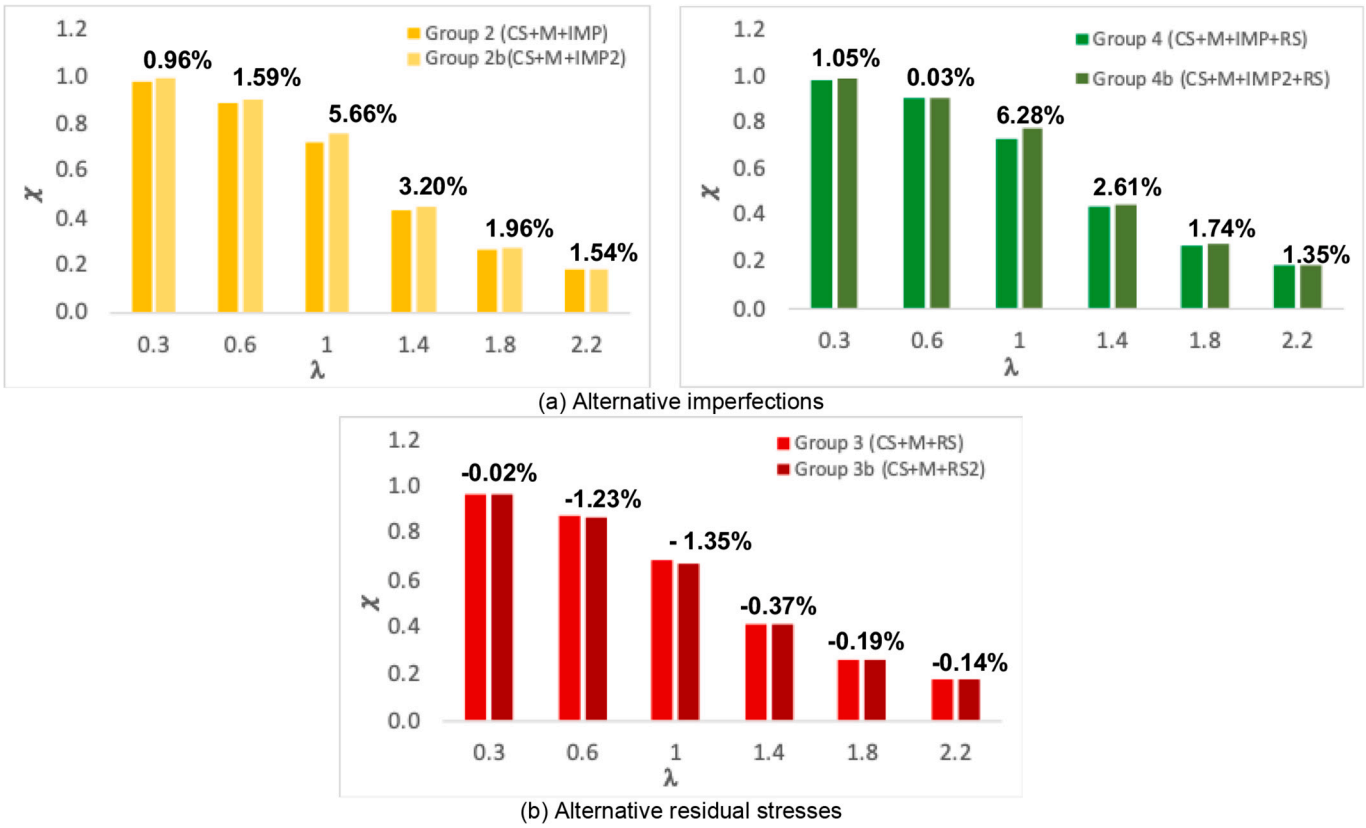


**Fig. 11.** Sensitivity study from the application of different statistical properties concerning the amplitude of the (a) initial geometric imperfections and (b) residual stresses.

**Table 13**
Comparison of the final resistance, $N_{b,Rd}$, between group 0 and EC3, group 1 and group 4 for minor-axis flexural buckling.

| SECTION | $\bar{\lambda}$ | Section Resistance (kN) | EC3* | group 0* | group 1** | group 4** | EC3/group0 |
|---|---|---|---|---|---|---|---|
| HE 300 A | 0.3 | 7057.5 | 0.96 | 1.01 | 1.08 | 1.09 | 0.95 |
| | 0.6 | | 0.80 | 0.91 | 1.08 | 1.12 | 0.88 |
| | 1.0 | | 0.57 | 0.71 | 1.08 | 1.17 | 0.81 |
| | 1.4 | | 0.38 | 0.44 | 1.06 | 1.11 | 0.86 |
| | 1.8 | | 0.26 | 0.29 | 1.03 | 1.06 | 0.89 |
| | 2.2 | | 0.18 | 0.19 | 1.07 | 1.10 | 0.96 |
| IPE 160 | 0.3 | 1243.36 | 0.95 | 1.04 | 1.09 | 1.09 | 0.92 |
| | 0.6 | | 0.80 | 0.94 | 1.08 | 1.10 | 0.86 |
| | 1.0 | | 0.57 | 0.71 | 1.06 | 1.15 | 0.81 |
| | 1.4 | | 0.38 | 0.45 | 1.03 | 1.08 | 0.84 |
| | 1.8 | | 0.25 | 0.28 | 1.05 | 1.08 | 0.91 |
| | 2.2 | | 0.18 | 0.19 | 1.03 | 1.05 | 0.93 |
| HE 280 M | 0.3 | 16,230.18 | 0.95 | 0.98 | 1.08 | 1.09 | 0.97 |
| | 0.6 | | 0.79 | 0.88 | 1.08 | 1.10 | 0.90 |
| | 1.0 | | 0.55 | 0.67 | 1.08 | 1.16 | 0.81 |
| | 1.4 | | 0.35 | 0.41 | 1.08 | 1.13 | 0.88 |
| | 1.8 | | 0.24 | 0.26 | 1.06 | 1.09 | 0.91 |
| | 2.2 | | 0.17 | 0.18 | 1.05 | 1.07 | 0.94 |
| HL 1100 M | 0.3 | 31,532.84 | 0.95 | 1.04 | 1.09 | 1.11 | 0.91 |
| | 0.6 | | 0.80 | 0.97 | 1.11 | 1.14 | 0.82 |
| | 1.0 | | 0.59 | 0.78 | 1.04 | 1.12 | 0.76 |
| | 1.4 | | 0.39 | 0.46 | 1.06 | 1.10 | 0.86 |
| | 1.8 | | 0.27 | 0.29 | 1.05 | 1.07 | 0.91 |
| | 2.2 | | 0.19 | 0.20 | 1.07 | 1.10 | 0.97 |
| HL 1500 M | 0.3 | 32,009.78 | 0.96 | 1.07 | 1.08 | 1.09 | 0.89 |
| | 0.6 | | 0.82 | 1.02 | 1.08 | 1.10 | 0.81 |
| | 1.0 | | 0.62 | 0.84 | 1.07 | 1.16 | 0.74 |
| | 1.4 | | 0.45 | 0.55 | 1.01 | 1.07 | 0.81 |
| | 1.8 | | 0.31 | 0.35 | 1.04 | 1.07 | 0.89 |
| | 2.2 | | 0.22 | 0.23 | 1.09 | 1.12 | 0.98 |
| HD 400 | 0.3 | 104,126.40 | 0.96 | 0.98 | 1.19 | 1.24 | 0.98 |
| | 0.6 | | 0.80 | 0.87 | 1.19 | 1.30 | 0.91 |
| | 1.0 | | 0.56 | 0.67 | 1.17 | 1.38 | 0.84 |
| | 1.4 | | 0.37 | 0.42 | 1.13 | 1.24 | 0.89 |
| | 1.8 | | 0.25 | 0.26 | 1.15 | 1.23 | 0.98 |
| | 2.2 | | 0.18 | 0.18 | 1.13 | 1.17 | 1.00 |
| | | Mean: | | | 1.08 | 1.13 | 0.89 |

* Results normalized with respect to cross-section resistance.
** Results normalized with respect to group 0.

axis buckling, respectively), the larger differences being observed for intermediate slenderness.

Comparing groups 1 and 4 to the Group 0, higher values are found (5% and 9% on average, for minor- and major-axis buckling, respectively) as more variables are considered as random. Concerning the variability of results, Figs. 12 and 13 show the results of the MC simulations, in which the mean, standard deviation and max and min values of each group are illustrated, normalized to the EC3 results. Comparing groups 1 and 4, a small increase of the average c.o.v is observed (from 3.0% to 4.6%, for minor-axis buckling, and from 2.4% to 3.8%, for major-axis buckling).

It can be concluded that the consideration of all basic variables as random leads to higher resistance with similar scatter. This supports the conclusion that it is safe to carry out reliability assessments with appropriate deterministic reference values for the amplitude of the initial bow imperfection and the amplitude of the residual stresses, as done in the recent investigation on the reassessment of buckling curves for the flexural buckling of HSS columns that were based on reliability studies that were validated with the consideration of only the material properties and the cross-section geometry as random variables [18].

## 5. Reliability assessment

The objective of this section is to assess the failure probability of current design rules available in Eurocode 3 [1,2,13] and the proposed design rules presented in proposal amendment available in refs. [18, 32] for the flexural buckling of HSS columns and compare it with the target probability of failure specified in EN 1990 [33]. Following the guidance from the SAFEBRICTILE project [12], appropriate subsets of cross sections and slenderness were considered, leading to the determination of the required partial factor $\gamma_{M1}$*. It is important to emphasize that the superscript "*" is used to indicate that this value is not a code value, but a computational result to be used as basis of the code value. This assessment is carried out firstly for minor-axis flexural buckling and then for major-axis flexural buckling by calculating, for each subset, the 0.118% quantile.

### 5.1. Reliability in the structural Eurocodes

The Eurocodes rely on a probabilistic framework [33] (Fig. 14) to establish design rules that satisfy a pre-defined target probability [55]. This evaluation must include uncertainties in material properties, geometrical properties, imperfections, and the design procedure itself [34]. Including all these variabilities in a probabilistic analysis is still nowadays difficult and very time consuming because the size of the samples would be in the range of $10^7$. The reliability framework document of the Eurocodes is EN 1990 – *Basis of structural design.* It establishes principles and requirements for the safety assessment of structures; it describes the basis of their design and provides guidelines for structural reliability.

The level of safety in EN 1990 is chosen according to Consequence classes (CC) defined in Annex B. The consequence classes establish the reliability differentiation of the code by considering the consequence of failure or malfunction of the structure. The Consequence Classes (CC)

**Table 14**
Comparison between group 0 and EC3, group 1 and group 4 for major-axis flexural bucking resistance.

| SECTION | λ | Section Resistance | EC3* | group 0* | group 1** | group 4** | EC3/group0 |
|---|---|---|---|---|---|---|---|
| HE 300 A | 0.3 | 7057.5 | 0.97 | 1.00 | 1.07 | 1.09 | 0.97 |
| | 0.6 | | 0.85 | 0.90 | 1.08 | 1.21 | 0.95 |
| | 1.0 | | 0.63 | 0.71 | 1.09 | 1.27 | 0.89 |
| | 1.4 | | 0.41 | 0.45 | 1.07 | 1.16 | 0.93 |
| | 1.8 | | 0.28 | 0.29 | 1.03 | 1.08 | 0.95 |
| | 2.2 | | 0.19 | 0.19 | 1.08 | 1.11 | 1.02 |
| IPE 160 | 0.3 | 1243.36 | 0.97 | 1.03 | 1.09 | 1.11 | 0.94 |
| | 0.6 | | 0.86 | 0.93 | 1.08 | 1.23 | 0.92 |
| | 1.0 | | 0.64 | 0.74 | 1.07 | 1.25 | 0.87 |
| | 1.4 | | 0.42 | 0.47 | 1.03 | 1.12 | 0.89 |
| | 1.8 | | 0.28 | 0.29 | 1.05 | 1.10 | 0.96 |
| | 2.2 | | 0.20 | 0.20 | 1.03 | 1.07 | 0.97 |
| HE 280 M | 0.3 | 16,230.18 | 0.96 | 0.97 | 1.08 | 1.11 | 0.99 |
| | 0.6 | | 0.82 | 0.86 | 1.08 | 1.21 | 0.95 |
| | 1.0 | | 0.56 | 0.68 | 1.09 | 1.26 | 0.83 |
| | 1.4 | | 0.35 | 0.41 | 1.09 | 1.17 | 0.85 |
| | 1.8 | | 0.23 | 0.26 | 1.06 | 1.11 | 0.86 |
| | 2.2 | | 0.16 | 0.18 | 1.05 | 1.09 | 0.87 |
| HL 1100 M | 0.3 | 31,532.84 | 0.96 | 1.17 | 1.09 | 1.11 | 0.82 |
| | 0.6 | | 0.85 | 1.04 | 1.08 | 1.23 | 0.82 |
| HL 1500 M | 0.3 | 32,009.78 | 0.96 | 1.34 | 1.06 | 1.09 | 0.72 |
| | 0.6 | | 0.86 | 1.20 | 1.09 | 1.18 | 0.72 |
| HD400 | 0.3 | 104,126.40 | 0.97 | 0.97 | 1.19 | 1.23 | 1.00 |
| | 0.6 | | 0.85 | 0.86 | 1.19 | 1.38 | 0.99 |
| | 1.0 | | 0.62 | 0.68 | 1.18 | 1.38 | 0.93 |
| | 1.4 | | 0.41 | 0.42 | 1.14 | 1.22 | 0.97 |
| | | Mean: | | | 1.09 | 1.18 | 0.91 |

* Results normalized with respect to cross-section resistance.
** Results normalized with respect to group 0.

correspond to Reliability classes (RC), which define the target reliability level through the reliability index $\beta$. This index defines the probability of failure, $P_f$, given by Eq. (10):

$$P_f = \Phi(-\beta) \tag{10}$$

where $\Phi$ is the cumulative distribution function (CDF) for the standard normal distribution.

The probability of failure, $P_f$, can also be simply expressed by Eq. (11), where $S$ is a linear limit state function described by Eq. (12). It is an approximation because in general the limit state function is non-linear, in which R and E represents the resistance and action variables, respectively.

$$P_f = Prob(S \leq 0) \tag{11}$$

$$S = \mathrm{R} - \mathrm{E} \tag{12}$$

The calculation of the probability of failure, $P_f$, includes both action and resistance variables. However, since they are assumed as uncorrelated variables, the First-Order Reliability Method (FORM) approach allows them to compute their scatter separately through the sensitivity factors $\alpha_E$ and $\alpha_R$, which give the relative importance of the individual random variables $E$ and $R$, respectively, for the definition of the reliability index, $\beta$, and follow the relation indicated in Eq. (13):

$$\sqrt{{\alpha_E}^2 + {\alpha_R}^2} \approx 1.0 \tag{13}$$

The sensitivity factors $\alpha_E$ and $\alpha_R$ are assumed to have the fixed values of $-0.7$ and 0.8 [33], respectively, for standard deviations of action, $E$, and resistance, $R$, that satisfy $0.16 < \sigma_E/\sigma_R < 7.6$.

It is noteworthy to state that an assessment considering both loading and resistance sides of the reliability was not done herein because the amount of work required (in terms of the number of simulations) would be unfeasible.

Consequently, the probability of failure related to the resistance side can be estimated according to Eq. (14):

$$P(R \leq r_d) = \Phi(-\alpha_R\beta) = \Phi(-0.8\beta) \tag{14}$$

in which $r_d$ represents the design value of the resistance.

Considering Consequence Class 2 with a design life of 50 years, $\beta$ assumes the value of 3.8 according to the specifications of EN 1990 [33], leading to $\Phi(-0.8\,x\,3.8) = \Phi(-3.04) = 0.00118$, which corresponds to the 99.8% percentile. This value can be alternatively approximated to the corresponding quantile of the resistance obtained from many simulations considering the Monte Carlo method, i.e. the design values of the resistance, $r_d$.

Once the design values,$r_d$, are defined, the required partial factors, ${\gamma_{M1}}^*$, can be obtained from Eq. (15), in which $r_k$is the characteristic value or alternatively the theoretical value (from specific design rules [2,32]) of the resistance.

$${\gamma_{M1}}^* = \frac{r_k}{r_d} \tag{15}$$

### 5.2. Minor axis flexural buckling

The required partial factors were calculated based on the design values obtained, which include the randomness of the relevant basic variables according to each group of samples considered (Fig. 15). This was done to evaluate whether the current design rules from EN 1993–1-1 [2] are in line with the target reliability level proposed by EN 1990 [33].

The partial factor for the resistance of members to instability, $\gamma_{M1}$, recommended by the Eurocode 3 [2] is equal to 1.0. Analysing the required partial factors obtained herein, it is observed that they lead to a value lower than unity, which confirms the conclusion that $\gamma_{M1}$ from the code is conservative.

Considering the recent proposal of Tankova et al. [18] to predict the minor-axis flexural buckling resistance of HSS columns, which is available in a forthcoming amendment [32] to FprEN 1993–1-1 [13], Fig. 16 shows the corresponding required partial factors.

Table 15 summarizes the required ${\gamma_{M1}}^*$ for the current version of EC3 [2] and the proposed amendment [32] for minor axis flexural buckling and compares the results of the assessment with all basic variables assumed as random (Group 4) with only material properties and cross

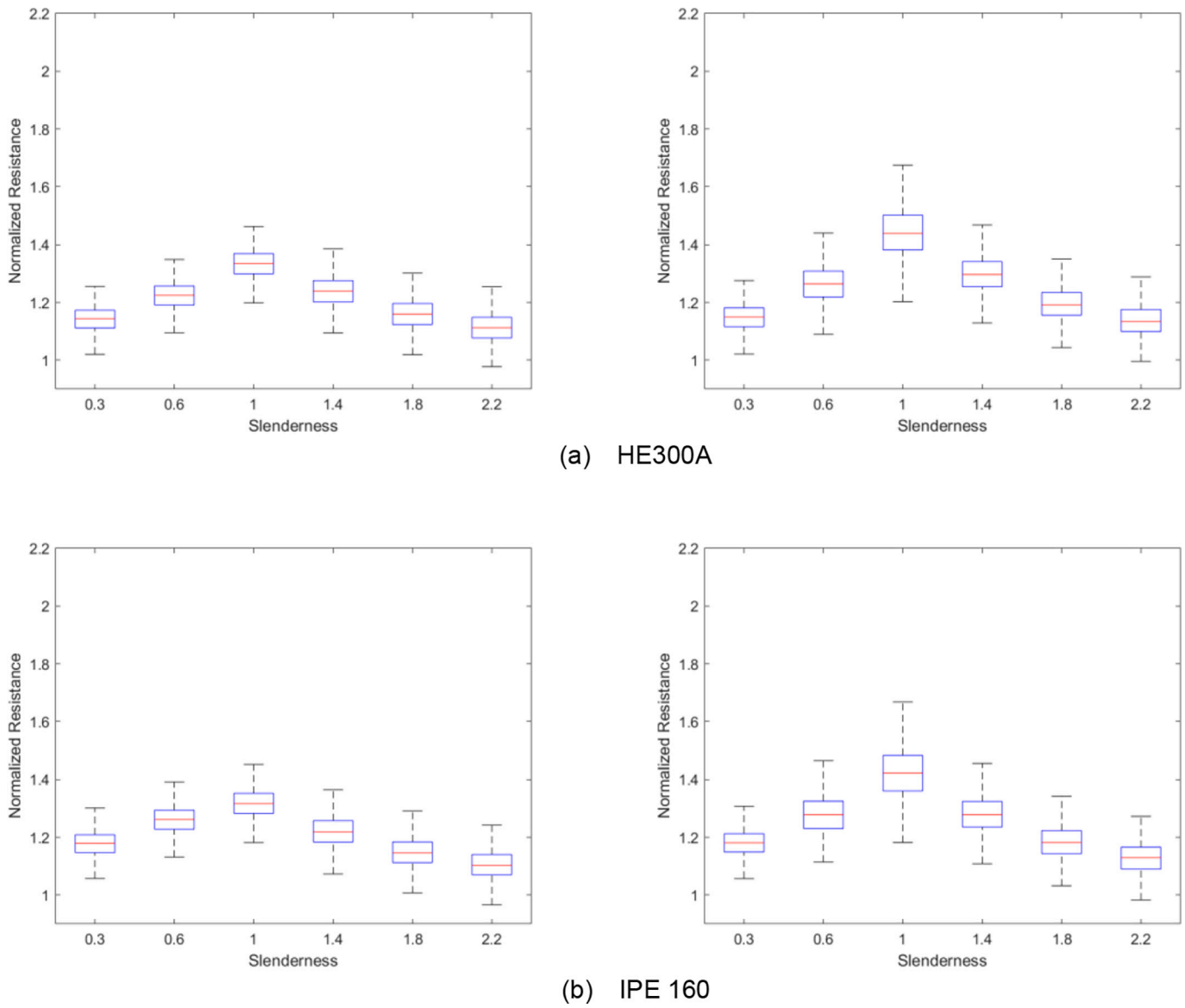


**Fig. 12.** Statistical results for minor-axis buckling from groups 1 and 4 displayed side by side (left and right charts, respectively).

section geometry assumed as random (Group 1). Using the higher buckling curve "b" as suggested in [32] leads to required partial factors closer to unity, therefore achieving a lower scatter across the different cases. The beneficial effect of considering all basic variables as random is again shown.

### 5.3. Major axis flexural buckling

For major axis flexural buckling, using a similar procedure as for minor axis leads to the required partial factors $\gamma_{M1}$* of Fig. 17 and Fig. 18 for the EC3 [2] design rules and the EC3 HSS amendment, respectively. The same conclusions are observed: EC3 leads to conservative results for both sets, while the amendment leads to required partial factors closer to unity, as exhibited in Table 16.

Table 16 provides a summary of the required $\gamma_{M1}$* values for the current version of EC3 [2] and the proposed amendment [32] concerning major axis flexural buckling. The comparison involves assessing results with all basic variables treated as random (Group 4), and only material properties and cross-section geometry assumed as random (Group 1). Adopting the higher buckling curve "b," as recommended in [32], results in required partial factors that are closer to unity, thereby reducing variability across different cases. Once again, this underscores the advantageous impact of considering all basic variables as random.

In Tankova et al. [18], required partial factors, $\gamma_{M1}$*, were also obtained considering the geometrical and material properties as random variables. Hence, it should exactly correspond to the results of Group 1 using the EC3 HSS amendment [32] from the Tables 15 and 16. However, the results are different: in the case of minor-axis flexural buckling, 1.036 and 0.977 are found instead of 0.998 and 0.914, for $t_f \leq 40\ mm$ and $t_f > 40\ mm$, respectively, and in the case of major-axis flexural buckling, 1.056 and 0.988 instead of 1.011 and 0.922, for $t_f \leq 40\ mm$ and $t_f > 40\ mm$, respectively. It is justified because the sample of simulations used in [18] is different from the current parametric study; three steel grades (S460, S500 and S690) are comprised by Tankova et al. [18] while this study only covers S690 (it is known that higher steel grades result in higher buckling resistance and consequently lower $\gamma_{M1}$*), and the reliability assessment in Tankova et al. [18] was carried out using the Annex D/SAFEBRICTILE procedure [12,33], instead of a full Monte Carlo simulation.

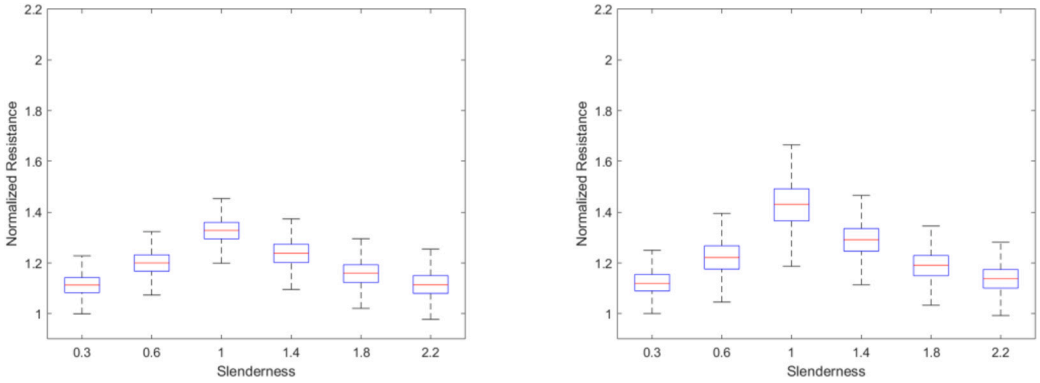


(c) HE 280 M

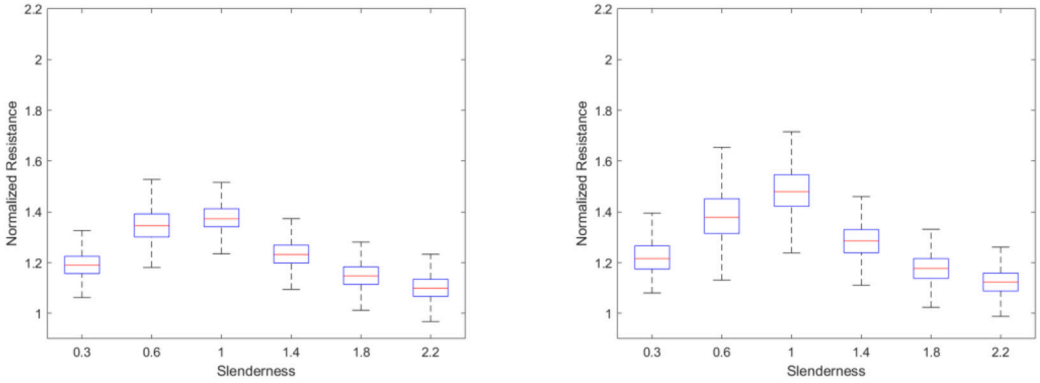


(d) HL 1100 M

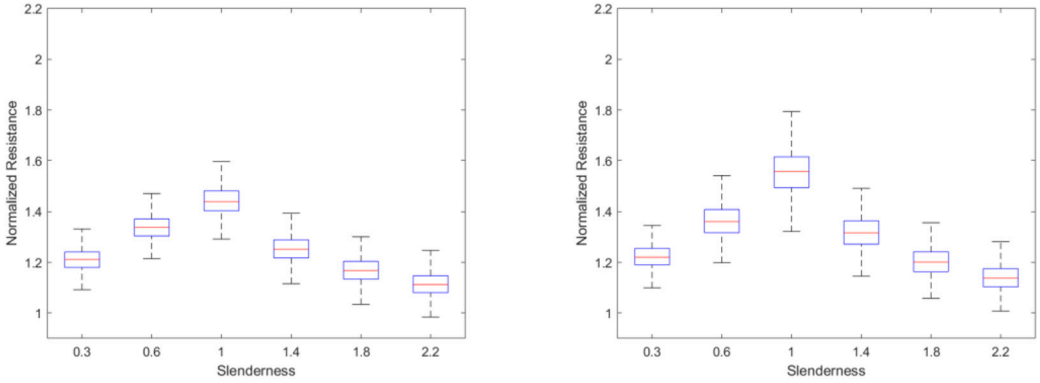


(e) HL 1500 M

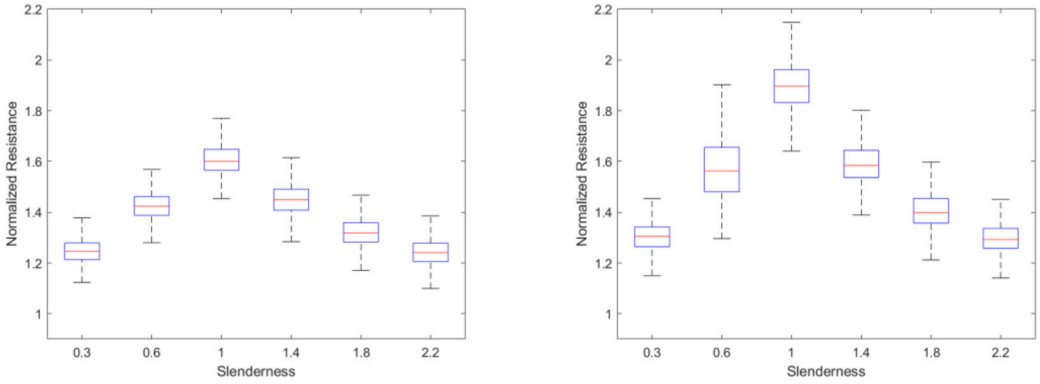


(f) HD 400

**Fig. 12.** (*continued*).

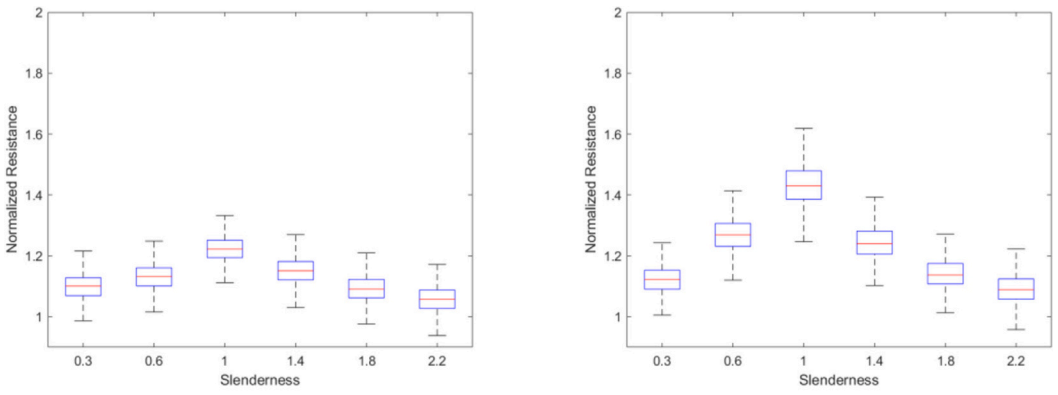


(a) HE300A

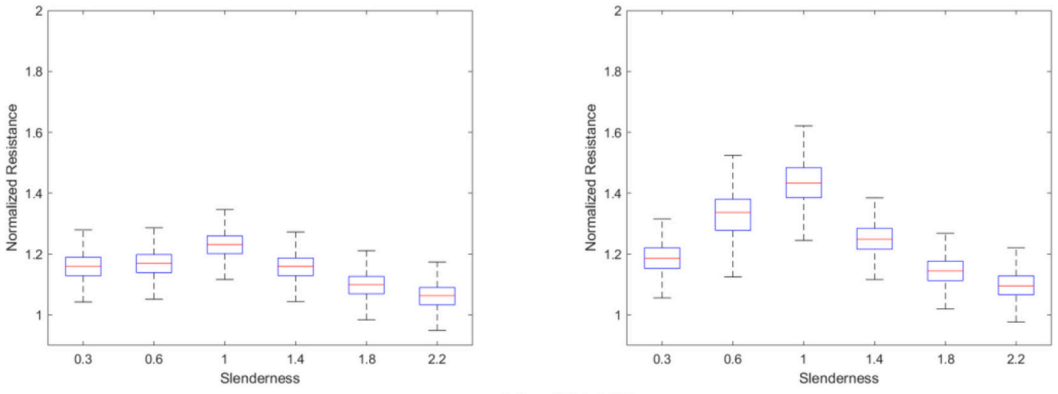


(b) IPE 160

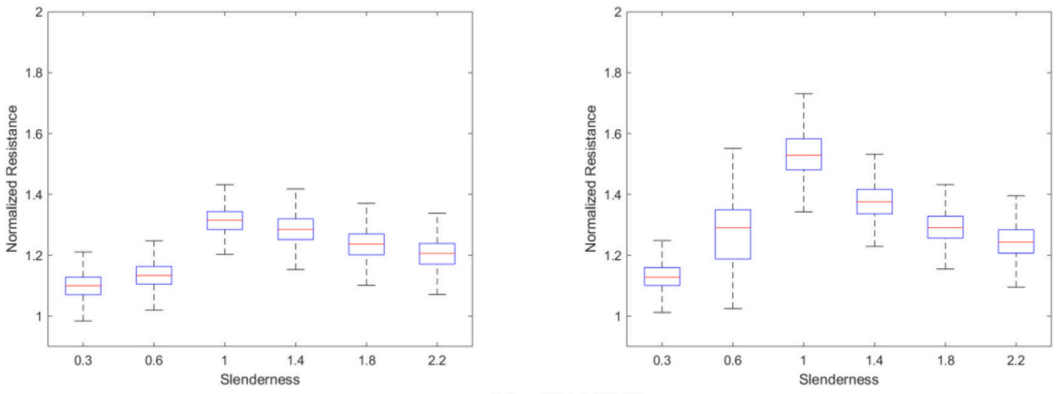


(c) HE 280 M

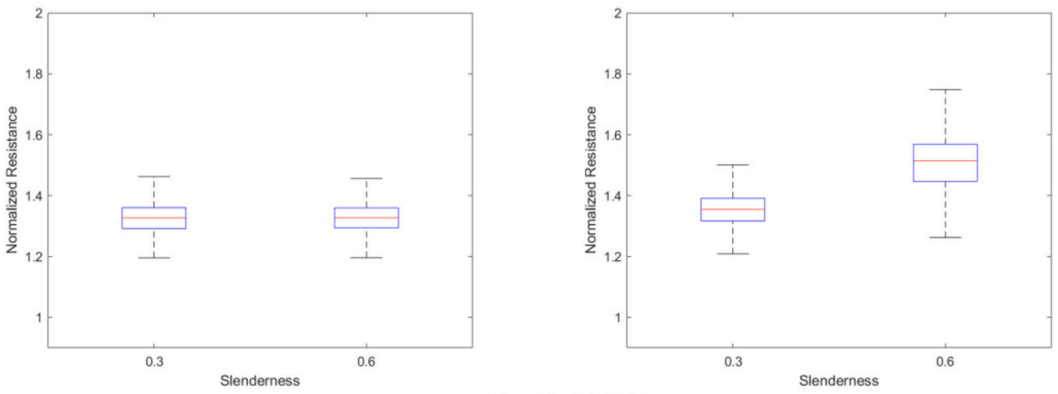


(d) HL 1100 M

**Fig. 13.** Statistical results for major-axis buckling from groups 1 and 4 displayed side by side (left and right charts, respectively).

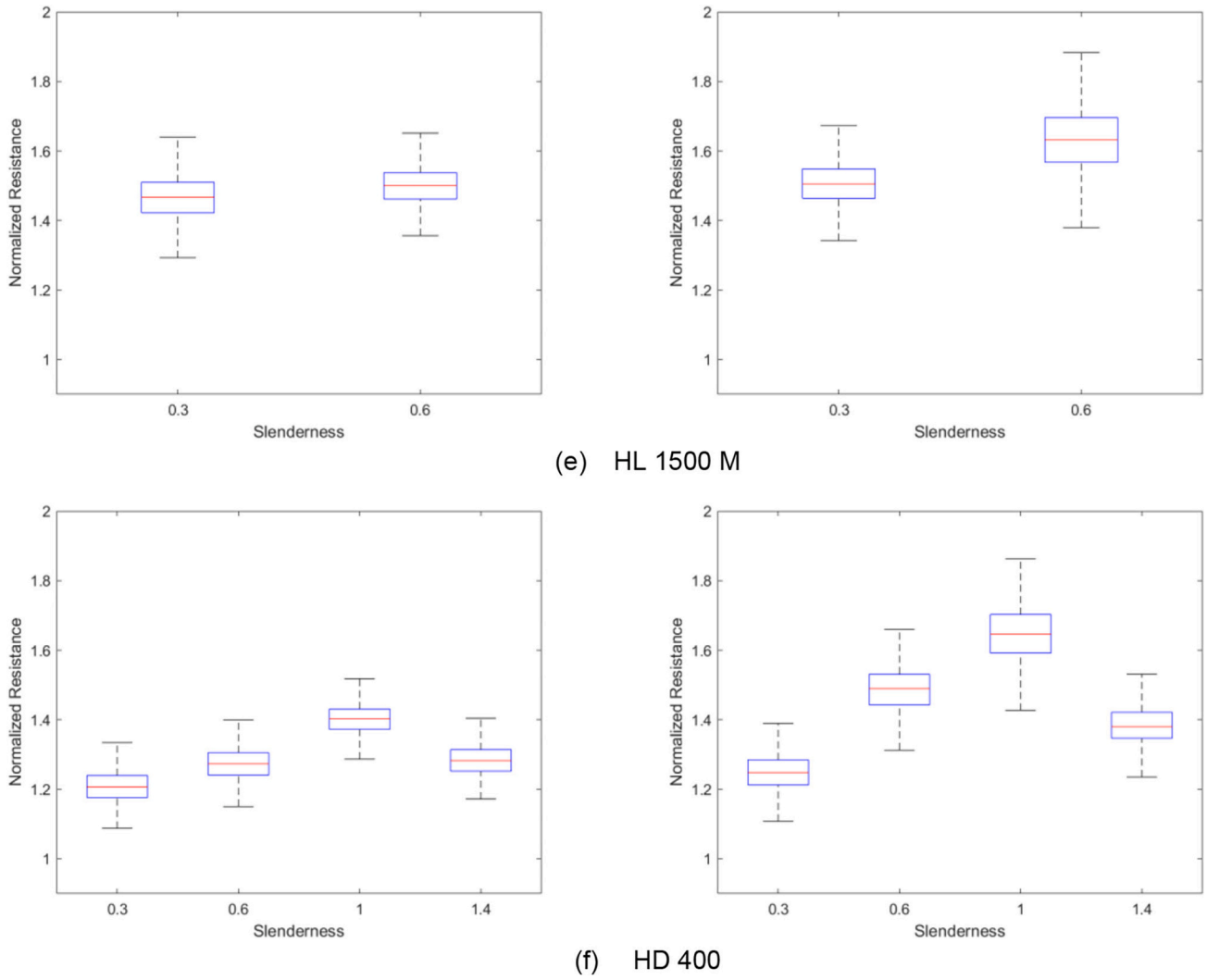


**Fig. 13.** (*continued*).

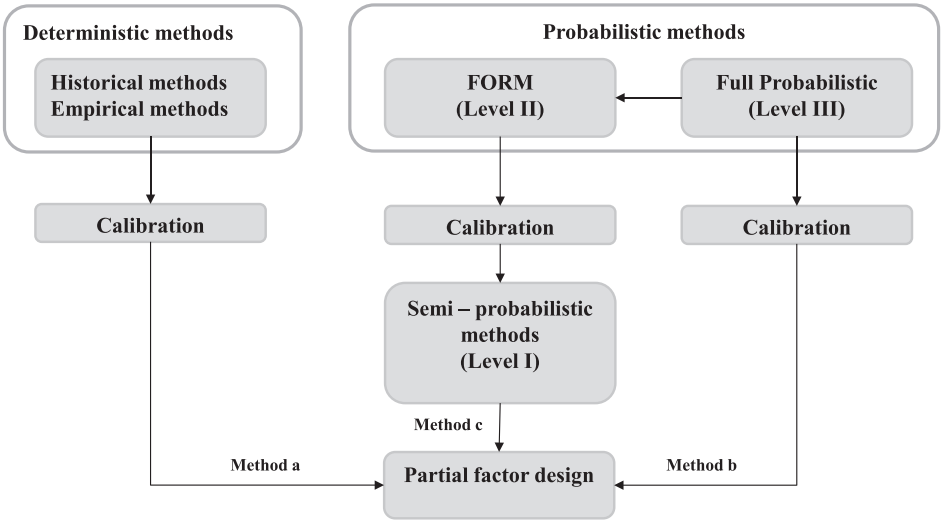


**Fig. 14.** Probabilistic framework of the Eurocodes.

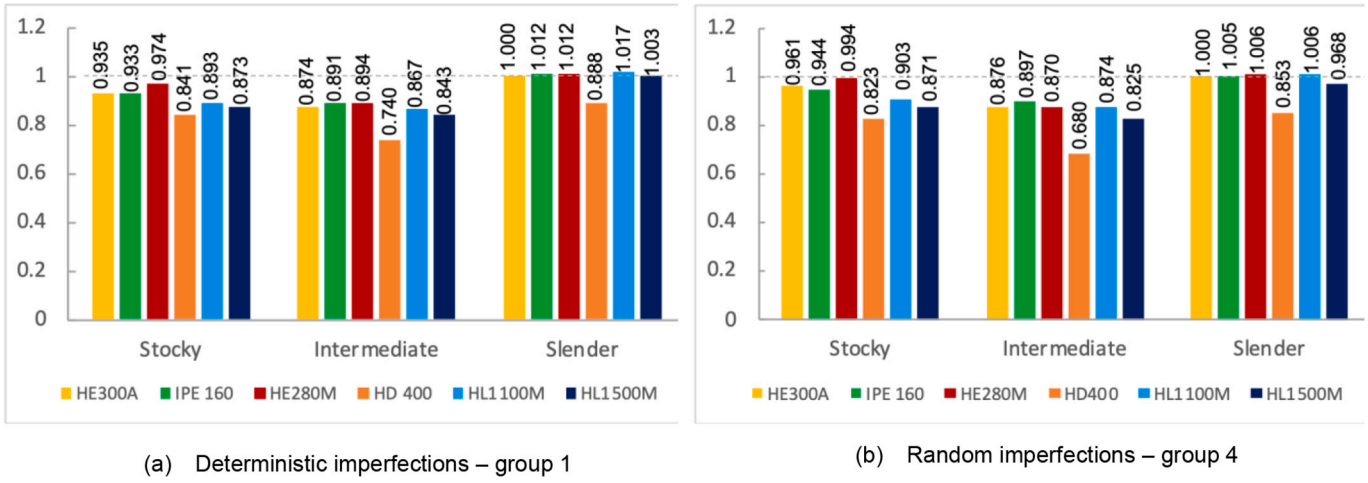


(a) Deterministic imperfections – group 1 (b) Random imperfections – group 4

**Fig. 15.** Required partial factors related to the Eurocode 3 [2] design rules for the minor-axis flexural buckling.

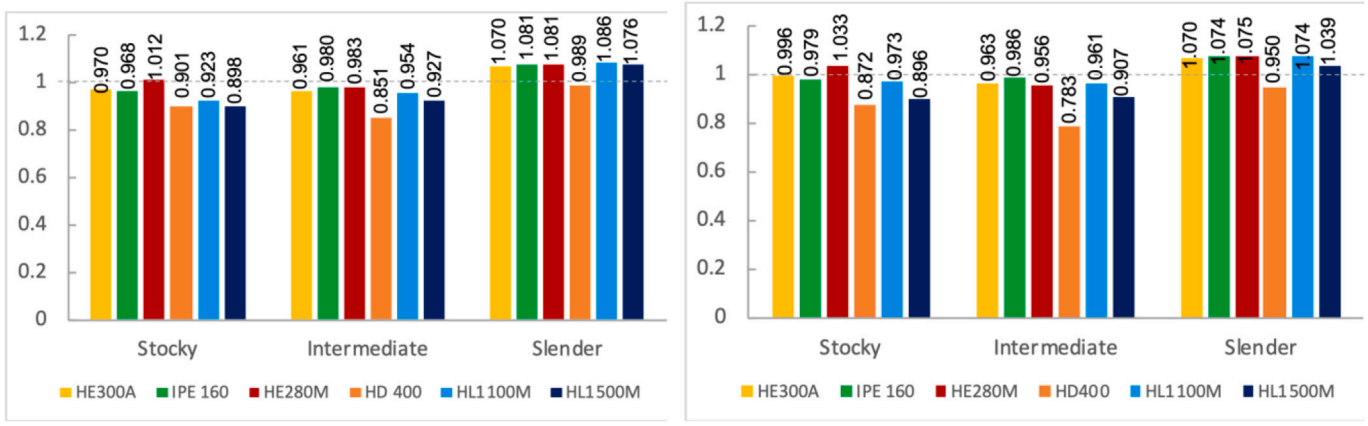


(a) Deterministic imperfections – group 1 (b) Random imperfections – group 4

**Fig. 16.** Required partial factors related to the curve proposed by EC3 HSS amendment [32] for the minor-axis flexural buckling.

**Table 15**
Required partial factors $\gamma_{M1}$*for minor axis flexural buckling.

| | | Slenderness | EC3 [2] | EC3 HSS amendment [32] |
|---|---|---|---|---|
| Group 1 | $t_f \leq 40\ mm$ | Low | 0.922 | 0.954 |
| | | Medium | 0.874 | 0.961 |
| | | High | 1.009 | 1.079 |
| | | ***Global*** | **0.935** | **0.998** |
| | $t_f > 40\ mm$ | Low | 0.841 | 0.901 |
| | | Medium | 0.740 | 0.851 |
| | | High | 0.888 | 0.989 |
| | | ***Global*** | **0.823** | **0.914** |
| Group 4 | $t_f \leq 40\ mm$ | Low | 0.935 | 0.975 |
| | | Medium | 0.868 | 0.955 |
| | | High | 0.997 | 1.066 |
| | | ***Global*** | **0.933** | **0.999** |
| | $t_f > 40\ mm$ | Low | 0.823 | 0.872 |
| | | Medium | 0.680 | 0.783 |
| | | High | 0.853 | 0.950 |
| | | ***Global*** | **0.785** | **0.868** |

## 6. Conclusions

In this study, Monte Carlo simulations were conducted using an advanced finite element model to assess the reliability of the flexural buckling behaviour of HSS welded I-section columns. Initial benchmarks indicated that 1000 column members were sufficient to estimate flexural buckling resistance; the global buckling imperfection led to the critical results rather than the local imperfection shape, or the combination of both, and the differences in the final resistance using different residual stress distribution due to the cutting process are negligible (around 1%). The study involved sensitivity analyses to compare the influence of the number of the random variables and the statistical parameters used to vary them, from which group of samples were selected to estimate the failure probability according to Eurocode 0 [33]. In the end, required partial factors were calculated based on a full-probabilistic approach, which had not been done in the literature so far, and used to assess the current Eurocode 3 [1,2,13] rules and the proposed amendment [32] to FprEN1993–1-1 [13]. The following conclusions could be achieved:

- it is safe-sided to carry out a reliability assessment only considering material properties and the cross-section geometry as random variables. Analysing the HE300A-section column, a beneficial effect for the resistance was found when the geometric imperfections are random (up to 1.4% of difference), a safe-side effect when the residual stresses are random (up to 1.3% of difference), and a beneficial effect when all basic variables are taken as random (up to 2.1% of difference). These trends were consistent across the other section columns and higher resistance was found when the imperfections were also taken as random. This conclusion supports that future reliability assessments can safely adopt the simplification of considering the imperfections as deterministic;

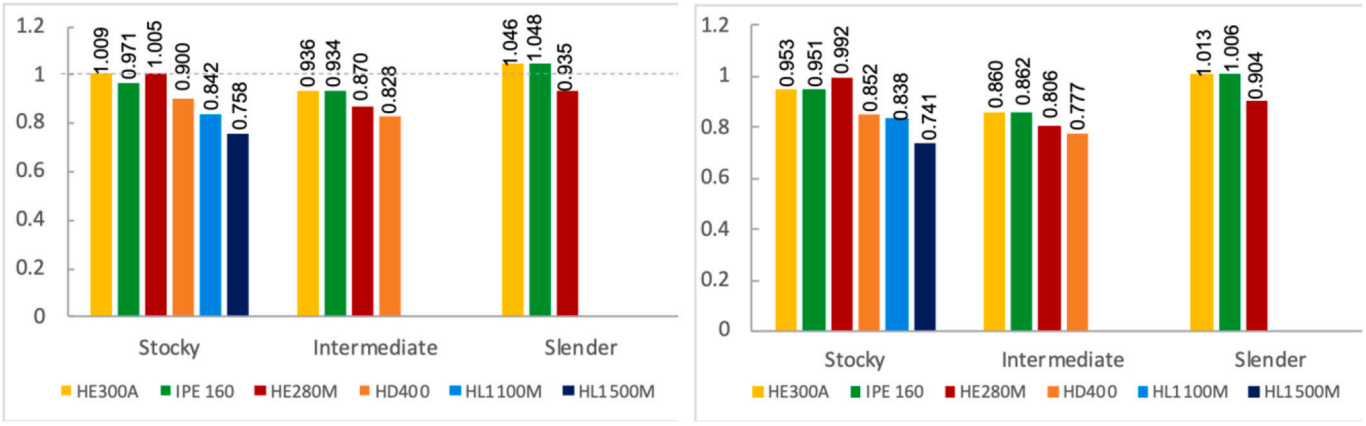


(a) Deterministic imperfections – group 1 (b) Random imperfections – group 4

**Fig. 17.** Partial safety factors related to the Eurocode 3 [2] design rules for the major-axis flexural buckling.

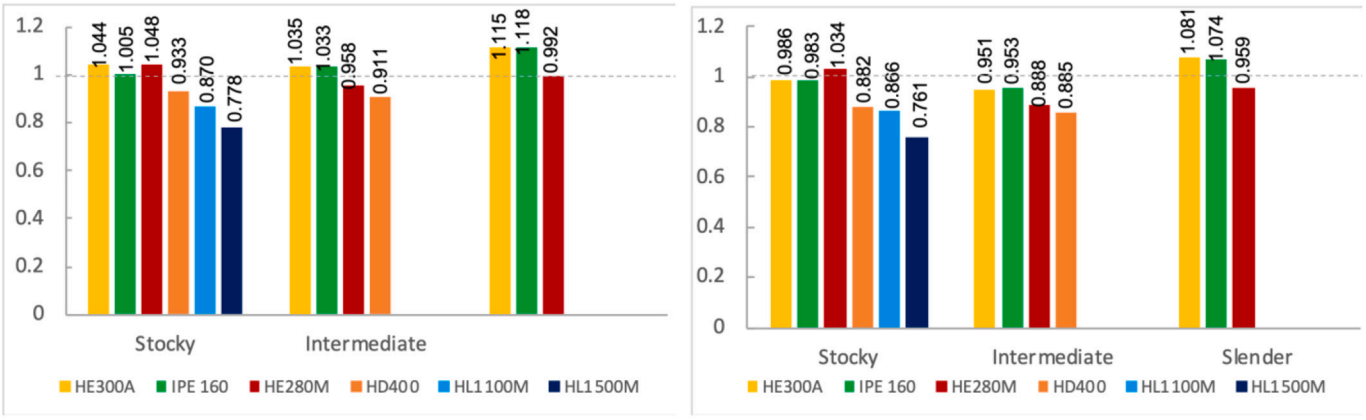


(a) Deterministic imperfections – group 1 (b) Random imperfections – group 4

**Fig. 18.** Partial safety factors related to the curve proposed in the EC3 HSS amendment [32] for the minor-axis flexural buckling.

**Table 16**
Required partial factors $\gamma_{M1}$*for major axis flexural buckling.

| | | Slenderness | EC3 [2] | EC3 HSS amendment [32] |
|---|---|---|---|---|
| Group 1 | $t_f \leq 40\ mm$ | Low | 0.917 | 0.949 |
| | | Medium | 0.914 | 1.009 |
| | | High | 1.010 | 1.075 |
| | | ***Global*** | **0.947** | **1.011** |
| | $t_f > 40\ mm$ | Low | 0.900 | 0.933 |
| | | Medium | 0.828 | 0.911 |
| | | High | | |
| | | ***Global*** | **0.864** | **0.922** |
| Group 4 | $t_f \leq 40\ mm$ | Low | 0.895 | 0.926 |
| | | Medium | 0.843 | 0.931 |
| | | High | 0.975 | 1.038 |
| | | ***Global*** | **0.904** | **0.965** |
| | $t_f > 40\ mm$ | Low | 0.852 | 0.882 |
| | | Medium | 0.777 | 0.855 |
| | | High | | |
| | | ***Global*** | **0.814** | **0.869** |

- it is safe-sided to carry out the simplified procedure Annex D [33] / SAFEBRICTILE [12] procedure instead of Monte Carlo simulations, for the same random variables (material properties and the cross-section geometry), which dramatically reduces the amount of work that is necessary to validate and assess the reliability of design methods for the buckling resistance of members (from hundreds of thousands to a few thousand);
- the current choice of buckling curves for welded profiles subject to compression in EN 1993–1-1 [2] and FprEN 1993–1-1 [13] is too conservative for steel grades larger than S460 and up to S700, with the reliability index $\beta$ well above the target value of 3.04 (resistance side only). For the minor-axis flexural buckling, the required partial factors, $\gamma_{M1}{}^{*}$, even assumed values equal to 0.933 and 0.785 (minor-axis flexural buckling) and 0.904 and 0.814 (major-axis flexural buckling), for flange thicknesses less or equal and superior to 40 mm, respectively, whilst using the proposal amendment [32] rules leads to required partial factors, $\gamma_{M1}{}^{*}$, closer to the unity for the same cases analysed. This validates the results of the STROBE project [15–18], which were established based on deterministic assumptions for the imperfections, and supports the ongoing proposals for the amendment [32].

## CRediT authorship contribution statement

**José Osvaldo Ferreira Filho:** Data curation, Formal analysis, Investigation, Software, Writing – original draft, Writing – review & editing. **Luís Simões da Silva:** Conceptualization, Investigation, Methodology, Supervision, Validation, Writing – original draft, Writing – review & editing. **Trayana Tankova:** Conceptualization, Methodology, Supervision, Validation, Writing – original draft, Writing – review &

editing. **Hermes Carvalho:** Supervision, Validation, Writing – review & editing.

## Declaration of competing interest

None.

## Data availability

Data will be made available on request.

## Acknowledgments

This work was partly financed by:

- FCT / MCTES through national funds (PIDDAC) under the R&D Unit Institute for Sustainability and Innovation in Structural Engineering (ISISE), under reference UIDB / 04029/2020 (https://doi.org/10.54499/UIDB/04029/2020), and under the Associate Laboratory Advanced Production and Intelligent Systems (ARISE) under reference LA/P/0112/2020.
- The doctoral grant 2021.06106.BD by the Portuguese Foundation for Science and Technology (FCT) attributed to the first author.

## References

[1] EN 1993-1-12, Eurocode 3: Design of steel structures – Part 1-12: Additional rules for the extension of EN 1993 up to steel grades S 700, European Committee for Standardization (CEN), 2007.
[2] EN 1993-1-1, Eurocode 3: Design of steel structures – Part 1-1: General rules and rules for buildings, European Committee for Standardization (CEN), 2005.
[3] ANSI/AISC 360-16, Specification for the Structural Steel Buildings, American Institute of Steel Construction (AISC), 2016.
[4] GB 50017, Standard for Design of Steel Structures, Chinese National Standards, 2017.
[5] D. Sfintesco, Fondement Expérimental des Courbes Européennes de Flambement, Construct. Métal. 3 (1970) 5–12.
[6] H. Beer, G. Schulz, Bases Théoriques des Courbes Européennes de Flambement, Construct. Métal. 3 (1970) 37–57.
[7] J. Strating, H. Vos, Simulation sur Ordinateur de la Coubre C.E.E.M de Flambement á l'aide de la Méthode de Monte-Carlo, Construct. Métal. no.2 (1973) 23–39.
[8] CTICM, Labein, ProfilARBED, RWTH, SCI, TNO, SAES, ECSC Steel RTD Programme - Partial safety factors for resistance of steel elements to EC3 and EC4 - Calibration for various steels products and failure criteria, Final report, European Communities, 2002. EUR 20344 EN.
[9] L.G. Cajot, M. Haller, Y. Conan, G. Sedlacek, O. Kraus, J. Rondla, F. Cerfontaine, B. Johansson, O. Lagerqvist, PROQUA – Probablistic quantification of safety of a steel structure highlighting the potential of steel versus other materials, Final report, Technical Steel Research, 2005 contract No. 7210-PR/249.
[10] C. Rebelo, N. Simões Lopes, L. da Silva, D. Vila Nethercot, P.M.M. Real, Statistical evaluation of the lateral-torsional buckling resistance of steel I-beams, part 1: variability of the Eurocode 3 resistance model, J. Constr. Steel Res. 65 (2009) 818–831.
[11] L. Simões da Silva, C. Rebelo, D. Nethercot, L. Marques, R. Vila Simões, P.M. M. Real, Statistical evaluation of the lateral-torsional buckling resistance of steel I-beams, part 2: variability of steel properties, J. Constr. Steel Res. 65 (2009) 832–849.
[12] Simões da Silva, L. Marques, L. Tankova, T. Rebelo, C. Kuhlmann, U. Kleiner, A. Spiegler, J. Snijder, R. Dehan Dkkler, V. Haremza, C. Taras, A. Cajot, L. G. Vassart, O. Popa, SAFEBRICTILE: Standardization of Safety Assessment Procedures Across Brittles to Ductils Failure Modes, Final Report. RFSR-CT-2013-00023, 2024.
[13] FprEN 1993-1-1, Eurocode 3: Design of steel structures – Part 1-1: General rules and rules for buildings, European Committee for Standardization (CEN), 2022.
[14] T. Tankova, L. Simões da Silva, L. Marques, C. Rebelo, A. Taras, Towards a standardized procedure for the safety assessment of stability design rules, J. Constr. Steel Res. 103 (2014) 290–302.
[15] N. Baddoo, M. Sansom, R. Pimentel, M. Lawson, A. Chen, F. Meza, L. Gardner, X. Yun, Y. Zhu, S. Schaffrath, H. Bartsch, F. Eyben, L. Simões da Silva, T. Tankova, F. Rodrigues, T. Lehnert, F. Gong, A. Dürr, Stronger Steels in the Built Environment (STROBE), RFSR-CT-2016-743504, 2021. Final Report.
[16] J.O. Ferreira Filho, T. Tankova, H. Carvalho, C. Martins, L. Simões da Silva, Experimental and numerical flexural buckling resistance of high strength steel columns and beam-columns, Eng. Struct. 265 (2022) 114414.
[17] T. Tankova, F. Rodrigues, C. Leitão, C. Martins, L. Simões da Silva, Lateral-torsional buckling of high strength steel beams: Experimental resistance, Thin-Walled Struct. 164 (2021) 107913.
[18] T. Simões Tankova, L. da Silva, F. Rodrigues, Buckling curve selection for HSS welded I-section members, Thin-Walled Struct. 177 (2022) 109430.
[19] T. Tankova, L. Simões da Silva, D. Rodrigues, M. Balukrishnam, H. Pasternak, B. Launert, T.Y. Tun, Residual stresses in welded I-section, Eng. Struct. 197 (2019) 109398.
[20] L. Schaper, T. Tankova, L. Simões da Silva, M. Knobloch, A novel residual stress model for welded I-sections, J. Constr. Steel Res. 188 (2022) 107017, https://doi.org/10.1016/j.jcsr.2021.107017.
[21] H. Ban, Y. Shi, Y. Wang, Overall buckling behavior of 460 MPa high strength steel columns: experimental investigation and design method, J. Constr. Steel Res. 74 (2012) 140–150.
[22] Wang, Y-B., Li, G-Q., Chen, S-W., Sun, F-F. (2012). Experimental and numerical study on the behavior of axially compressed high strength steel columns with H-section. Eng. Struct., 43, 149–159. 2024.
[23] F. Zhou, L. Tong, Y. Chen, Experimental and numerical investigations of high strength steel welded H-section columns, Int. J. Steel Struct. 13 (2) (2013) 209–218.
[24] K.J.R. Rasmussen, G.J. Hancock, Tests of high strength steel columns, J. Constr. Steel Res. 34 (1995) 27–52.
[25] G. Shi, H. Ban, F.S.K. Bijlaard, Tests and numerical study of ultra-high strength steel columns with end restraints, J. Constr. Steel Res. 70 (2012) 236–247.
[26] T.-J. Li, G.-Q. Li, S.-L. Chan, Y.-B. Wang, Behavior of Q690 high-strength steel columns: part 1: experimental investigation, J. Constr. Steel Res. 123 (2016) 18–30.
[27] T.-Y. Ma, Y.-F. Hu, X. Liu, G.-Q. Li, K.-F. Chung, Experimental investigation into high strength Q690 steel welded H-sections under combined compression and bending, J. Constr. Steel Res. 138 (2017) 449–462.
[28] T.-Y. Ma, X. Liu, Y.-F. Hu, K.-F. Chung, G.-Q. Li, Structural behaviour of slender columns of high strength S690 steel welded H-sections under compression, Eng. Struct. 157 (2018) 75–85.
[29] Y. Sun, Y. Liang, O. Zhao, Minor-axis flexural buckling behaviour and resistances of pin-ended S690 high strength steel welded I-section columns, Thin-Walled Struct. 156 (2020) 106980.
[30] H. Ban, G. Shi, Y. Shi, M.A. Bradford, Experimental investigation of the overall buckling behaviour of 960 MPa high strength steel columns, J. Constr. Steel Res. 88 (2013) 256–266.
[31] A. Su, Y. Sun, Y. Liang, O. Zhao, Experimental and numerical studies of S960 ultra-high strength steel welded I-sections under combined compression and minor-axis bending, Eng. Struct. 243 (2021) 112675.
[32] Simões da Silva, L. Knobloch, M. Tankova, T. Bours, A.-L. Schaper, Proposal for an amendment of EN 1993–1-1_HSS_v8. European Committee for Standardization – CEN/TC250/SC3/WG "Evolution of EN1993–1-1 – General rules for buildings", 2022.
[33] EN 1990, Eurocode – Basis of Structural Design, European Committee for Standardization (CEN), Brussels, 2002.
[34] A.H.-S. Ang, W.H. Tang, Probability Concepts in Engineering, 2nd edition, Wiley, 2007.
[35] EN 1993-1-5, Eurocode 3: Design of steel structures – Part 1–5: Plated structural elements, European Committee for Standardization (CEN), 2006.
[36] Abaqus, v.6.21, Dassault Systems/Simulia, Providence, RI, USA, 2021.
[37] X. Yun, L. Gardner, Stress-strain curves for hot-rolled steels, J. Constr. Steel Res. 133 (2017) 36–46.
[38] B. Braun, R. Chacon, H. Degée, Y. Duchêne, L. Dunai, L. Kovesdi, U. Kuhlmann, G. Lener, V. Pourostad, F. Sinur, R. Timmers, Design of Steel Plated Structures with Finite Elements, ECCS Press, Brussels, 2023.
[39] J.P. Martins, L. Simões da Silva, T. Tankova, H.D. Craveiro, Reliability assessment of EC3-1-5 methodology of welded slender cross-sections under direct stresses, J. Constr. Steel Res. 160 (2019) 301–319.
[40] D. Jindra, Z. Kala, J. Kala, Flexural buckling of stainless steel CHS columns: reliability analysis utilizing FEM simulations, J. Constr. Steel Res. 188 (2022) 107002.
[41] R. Landolfo, Material Ductility and Buckling Behaviour of Eurocode-compliant Cold-formed Steel Hollow Columns. c/e papers, 5, 4, 2024, pp. 1–8.
[42] ECCS, Ultimate Limit State Calculation of Sway Frames with Rigid Joints, Publication No.33, Brussels, 1984.
[43] Y. Fukumoto, Y. Itoh, Statistical study of experiments on welded beams, J. Struct. Div. 107 (ST1) (1981) 89–103.
[44] prEN 1993-1-14, Eurocode 3: Design of steel structures – Part 1–14: Design assisted by finite element analysis, European Committee for Standardization (CEN), 2022.
[45] T.-J. Li, G.-Q. Li, Y.-B. Wang, Residual stress tests of welded Q690 high-strength steel box- and H-sections, J. Constr. Steel Res. 115 (2016) 283–289.
[46] B. Zheng, S. Yang, X. Jin, G. Shu, S. Dong, Q. Jiang, Test on residual stress distribution of welded S600E high-strength stainless steel sections, J. Constr. Steel Res. 168 (2020) 105994.
[47] T. Le, A. Paradowska, M.A. Bradford, X. Liu, H.R. Valipour, Residual stresses in welded hihg-strength steel I-beams, J. Constr. Steel Res. 167 (2020) 105849.
[48] Z. Yang, W. Wang, J. Zhang, L. Xu, Effect of fire exposure on residual stresses relief in welded high strength Q690 steel sections, J. Constr. Steel Res. 177 (2021) 106455.
[49] D. Li, A. Paradowska, B. Uy, J. Wang, M. Khan, Residual stresses of box and I-shaped columns fabricated from S960 ultra-high-strength steel, J. Constr. Steel Res. 166 (2024) 105904.
[50] Y. Sun, Y. Liang, O. Zhao, Testing, numerical modelling and design of S690 high strength steel welded I-section stub columns, J. Constr. Steel Res. 159 (2019) 521–533.

[51] A. Su, Y. Sun, Y. Liang, O. Zhao, Material properties and membrane residual stresses of S690 high strength steel welded I-sections after exposure to elevated temperatures, Thin-Walled Struct. 152 (2020) 106723.
[52] A. Su, Y. Sun, Y. Liang, O. Zhao, Membrane residual stresses and local buckling of S960 ultra-high strength steel welded I-section stub columns, Thin-Walled Struct. 161 (2021) 107997.
[53] D.-K. Kim, C.-H. Lee, K.-H. Han, J.-H. Kim, S.-E. Lee, H.-B. Sim, Strength and residual stress evaluation of stub columns fabricated from 800 MPa high-strength steel, J. Constr. Steel Res. 102 (2014) 111–120.
[54] K. Pearson, On the criterion that a given system of deviations from the probable in the case of a correlated system of variables is such that it can be reasonably supposed to have arisen from random sampling, in: The London, Edinburgh and Dublin Philosophical Magazine and Journal of Science Series 5 50(302), 1900, 2009, pp. 157–175, https://doi.org/10.1080/14786440009463897.
[55] H. Gulvanessian, J.-A. Calgaro, M. Holicky, Designers' guide to EN 1990. Eurocode: Basis of Design, 2002.